Article

Not peer-reviewed version

Semiconductor and Liquid Assisted Photothermal Effect: A New Method to Generate Electricity from Sunlight

Ibram Ganesh *

Posted Date: 15 November 2023

doi: 10.20944/preprints202311.0965.v1

Keywords: Electricity generation from sunlight; SLAPE; SPVC; renewable and sustainable energy; -butyrolactone

Article

Semiconductor and Liquid Assisted Photothermal Effect: A New Method to Generate Electricity from Sunlight

Ibram Ganesh*

Centre of Excellence for Artificial Photosynthesis, International Advanced Research Centre for Powder Metallurgy and New Materials (ARCI), Balapur Post, Hyderabad – 500 005, Telangana, India.
*E-mail: ibramganesh@arci.res.in; dribramganesh@gmail.com; fax: +91-40-24442699)

Abstract: The *Semiconductor and Liquid Assisted Photothermal Effect (SLAPE)*" concept was employed for the first time in this study to generate electricity from sunlight. In SLAPE process, a semiconducting material is immersed completely in a stable organic solvent to capture the complete sunlight reaching the earth surface and to turn it into the heat-energy that can be eventually converted into electricity by using Organic Rankine Cycle (ORC) with the help of a heat engine and electric generator. In this investigation, the SLAPE solar panels were fabricated with two top and bottom chambers separated by thin thermally conducting metal sheet (Cu or Al). Multi-crystalline silicon photovoltaic cells (SPVCs) in conjunction with γ-butyrolactone were employed to capture the sunlight, and a low-boiling point dichloromethane (DCM) solvent was employed as a working fluid to capture the *in situ* generated heat energy from sunlight. Upon exposure to the natural sunlight, the 21 numbers of SPVCs together with about 2 litres γ-butyrolactone containing one square meter area SLAPE solar panel has generated about 17 V when integrated with a laboratory model reciprocally moved steam engine and a custom-made electric generator, whereas, a commercial SPVC solar panel with 21 number SPVCs generate a maximum voltage of 11 V. The theoretical background governing the SLAPE solar panels, the necessity for their invention and the proof of concept of SLAPE solar panels have been thoroughly presented and discussed and established in this article.

Keywords: electricity generation from sunlight; SLAPE; SPVC; renewable and sustainable energy; γ-butyrolactone

1. Introduction

1.1. The role of practicable artificial photosynthesis to achieve self-sufficiency in energy security and to solve the CO_2 associated global warming problem and the social cost of carbon

Today, the development of a simple, inexpensive and efficient process for producing electricity from sunlight, and use of that electricity to convert the waste-steam greenhouse CO_2 gas into energy rich solar-fuels, and to split water into H_2 and O_2 gases, which is popularly called as an "*Artificial Photosynthesis (AP)*" [1], have been considered as one of the top-most research priorities across the globe as these processes can solve the problems related to i) securing the self-sufficiency in energy production by each and every country, ii) the CO_2 associated global warming, and the resultant social cost of carbon, iii) the storing of renewable (and surplus) energy in an high-energy-density carbon-neutral liquid-fuels such as, methanol so that they can be directly employed in place of diesel and petrol in the present existing energy distribution infrastructure (i.e., in the *internal combustion (IC)* engines) so that there would not be any severe economic consequences while transforming from fossil fuel energy dependency to non-fossil fuel, renewable and solar energy dependency, and iv) depletion of fossil fuels mainly the crude oil, which is an important resource of several commodity chemicals required for the future generations [1-25]. Efficient sunlight-to-electricity conversion technology can eliminate up to 8-15% power transmission losses that are associated with the grid-connected electricity produced at remote places far from the densely populated cities by burning fossil fuels

(i.e., coal, natural gas and crude oil) at thermal power plants. In fact, as on today, the synthesis of liquid-fuels from CO_2, and, splitting of water into H_2 and O_2 gases using electricity derived from sunlight in electrochemical cells can be considered as one of the most effective, and economic way of storing energy to circumvent the daily and seasonal intermittency of solar energy as the energy stored in H_2 and O_2 gases or CO gas can be taken back again as and when required on a demand basis using fuel cells [1,10,12,26]. In fact, today, the fossil fuels are the main energy resource supplying to meet >85% of the primary energy requirement of all most all developed and developing countries except very few countries including France and Germany, and their usage has been found to be responsible for raising the concentrations of CO_2 in the atmosphere and for the resultant global warming as well as for the social cost of carbon problems [1,27-37].

It is a well-known fact that nature stores solar energy to feed not only 8 billion people but also the entire life living today on our planet in the natural photosynthesis (NP) process by using CO_2 and water as energy storing materials [1,4,8,38-47]. In fact, the NP process is nothing but the storing of solar energy by using CO_2 and water as energy storing materials by following a natural photosynthesis process in the form of food materials and bio-mass to feed human beings and animals. The solar energy stored in the form of food materials (i.e., grains) can be preserved and used as and when required on a demand basis. The natured stored solar energy in the form of food materials need not have to be used immediately like the electricity produced from sunlight by using SPVC solar panels needs to be used. Furthermore, the amount of solar energy stored by plant leaves in the form of food material and bio-mass in the NP process cannot be stored in any of the manmade existing energy storing devices including the most advanced lithium ion batteries and capacitors as it would be prohibitively expensive [1,10,12]. Nature clearly suggests that any amount of energy can be stored by using CO_2 and water as energy storing materials while beneficially contributing to the environment. In fact, the fossil fuels are nothing but solar energy stored by the nature. The fuel chemicals synthesized in AP by using electricity derived from sunlight are called as solar fuels, which are exactly similar to fossil fuels. The only difference between the fossil and solar fuels is the former ones are created by the nature from bio-mass in which the solar energy was stored by plant leaves using CO_2 and water as energy storing materials at the rate of 0.2%, whereas, the solar-fuels, have to be synthesized by following manmade technologies by electrochemically reducing CO_2 and splitting water using electricity derived from sunlight to meet all the energy needs of the society with a minimum (conversion) efficiency >10% so that these processes can be practiced at industry with economic viability. Hence, the entire energy distribution infrastructure available today to use fossil fuels can also be used for solar fuels formed in AP process as well. Thus, the renewable liquid-fuel chemicals produced from CO_2 gas in AP process can indeed replace the fossil fuels in all their current uses such as, powering industrial processes, machinery and transportation, etc.. In fact, the AP process can establish a closed-loop CO_2 cycle that turns the conventional fuels into the "green energy vectors". Furthermore, the energy density of electricity storing batteries is far too low for most of the power-intensive applications (about 1-2%) in comparison to those can be stored in carbon-based fuels (50 MJ/kg with methane, methanol, diesel and gasoline) [1,10,12]. In fact, the e-batteries such as Li-ion batteries are best suitable and opt for low-energy required portable devices such as, mobile phones, laptops, etc., but not for high-energy intensive applications such as, heavy duty vehicles, buses, lorries, trucks, aero planes, etc.. Furthermore, batteries also have certain limitations with respect to their cost, service life, recharging time, involvement of hazardous and polluting materials, etc..

Once a suitable and inexpensive method for converting sunlight into electricity is developed, and thus, obtained electricity is suitably utilized to convert the waste-stream greenhouse CO_2 gas into CO, and the water into H_2 and O_2 gases, all most all countries can use solar energy to meet all their energy requirements without depending on foreign countries to import the fossil fuels while meeting all the deadlines imposed by *Intergovernmental Panel on Climate Change (IPCC)* and *United Nations Framework Convention on Climate Change (UNFCCC)* as far as environmental safety and release of CO_2 gas into the atmosphere are concerned [1,18-22,24]. Upon implementing such an AP process worldwide, in about 10 to 15 years period, a lot of fossil fuels burned so far to meet the energy

requirement of the society can be restored in the form of natural gas at all the sea shores across the globe as no CO_2 is freshly released into the atmosphere in large quantities as CO_2 present in the atmosphere is consumed by the plant leaves so that its concentration will come down to those levels (i.e., about 280 ppm) present in the atmosphere prior to the industrial revolution started during period of around 1750 to early 1800 century. Once, this target is reached, the unseasonal and unexpected heavy rains and floods that are occurring these days can be minimized, which are disturbing the functioning of society for several days together in certain cities like those recently occurred in Chennai city in the year 2015 [48], and Kerala in the year 2018 [49].

In view of the above reasons, the development of a simple, easy to fabricate, and inexpensive method to produce electricity from sunlight, and using thus obtained electricity to drive the reactions of AP are of utmost important to solve both energy and environment related problems. For example, today, India alone has 118 thermal power plants, 220 cement industries, 650 steel plants (including those small scale industries), and 18 public sector refineries and 5 refineries in the private sector/or as a joint venture, the largest refineries being RIL Jamnagar (Gujarat), NEL Vadinar (Gujarat) and IOC Panipat (Haryana). All these industries together everyday generate several million tons of CO_2 gas by burning fossil fuels such as, oil, coal, and natural gas to meet the energy needs of the society, and all thus generated CO_2 gas is released into the atmosphere. Once, an inexpensive and simple to fabricate solar panels to produce electricity from sunlight are developed to drive the reactions of AP efficiently at lower processing cost, then by following that process all the CO_2 generated at major outlets across the globe can be converted into CO gas initially, and then into methanol, diesel and synthetic petrol [1,18-22,24]. The *IPCC* and *UNFCCC* are responsible for pledging 197 countries (as on December 2015) to take the responsibility to stabilize the greenhouse CO_2 gas concentration in the atmosphere at a level that would prevent dangerous anthropogenic interference with the climatic system. Furthermore, for example, according to *IPCC* and *UNFCCC* by 2030, the *European Union (EU)* has to meet ≥27% of their primary energy requirement from the renewable energy resources, which ensures up to 40% reduction in *greenhouse gas (GHGs)* emissions in comparison to 1990 levels [1,50-54]. Today, EU gets about 50% of its primary energy from the imported fossil fuels. In EU, the buildings are the leading consumers of energy (40%), ahead of transportation (32%), industry (27%) and agriculture (2%). Heating is at top of the consumption list accounting for 65% of domestic energy use. As a result, 33% of the total CO_2 emissions in EU come from fossil fuels used for heating purposes only. Only ~17% of the total energy requirement is met by the electricity and out of which about 11.7% is met from hydroelectric power.

There are two ways to control the CO_2 associated global warming problem. One is to replace the fossil fuels usage with renewable energy vectors such as, solar energy [1,10,12], and the other one is to find out the solutions to solve the CO_2 associated global warming problem [1,55-61]. Today, the readily available technology to solve the CO_2 associated global warming problem is the "*CO_2 sequestration*", which is also known as the "*carbon capture and storage (CCS)*" process. This latter process is not only expensive but also quite cumbersome. As a part of the CCS process, the CO_2 captured at various outlets such as, thermal power plants, cement industry, steel factories, gas refineries, etc., is transported and pumped mainly into the deep seawater below 3500 meters [55]. At 3500 meters deep in the sea, a pressure of >350 bar and a temperature of ~3°C exist. When CO_2 is exposed to these conditions, it turns into CO_2 clathrate, which is a snow-like crystalline substance, composed of H_2O ice and CO_2. Nevertheless, its long term stability is still a debatable subject. It is also a known fact that the CO_2 capturing sites are most often far away from those sites normally used for CO_2 sequestration. In certain places like those in Europe, CO_2 transportation in pipelines to the storage sites is quite difficult, and it will increase the cost of the process by at least 15-20%, which is considered to be unacceptable [1,10,12]. The *Department of Energy (DoE)*, USA, suggests that the transportation of CO_2 in tankers on road is not acceptable if the distance is more than 100 km. In the total CCS process, about 35-40% is the transportation and storage costs. This cost would be between 35 and 50 €/ton for early commercial phase and between 60 and 90 €/ton during demonstration phase, when transportation of CO_2 is made by pipelines for distances not over 200-300 km [10,12]. This cost would be further increased if the transportation is made by road (for example, in certain European

Preprints (www.preprints.org) | NOT PEER-REVIEWED | Posted: 15 November 2023 doi:10.20944/preprints202311.0965.v1

countries). Recently, a new CO_2 sequestration process was reported, in which when a mixture of water and CO_2 was pumped 540 meters deep into the Iceland rocks, this acidic solution causes the leaching of the Mg and Ca metals out of the basalt rocks and converts them into $MgCO_3$ and $CaCO_3$ rocks [62]. These latter rocks have been found to be stable for more than two-year period. The cost of this new CO_2 sequestration process has been estimated to be about 18 USD for disposing off a ton CO_2 gas. Thus, the CO_2 sequestration processes are not only expensive and laborious, they also irreversibly blocks the important C_1 carbon resource in the form of CO_2 cletherate in deep seawater, which cannot be used for any of the beneficial activities of the human beings. In fact, the CO_2 shall be participated in the natural carbon cycle that is required for the sustainability of the life on earth [47,63].

Alternatively, CO_2 can be converted into several value added chemicals and fuels in a process called "*carbon capture and utilization (CCU)*" with the same expenditure that can be incurred for the CCS process [1-3,64]. Sometimes, the value of the product(s) formed in the CCU process can become a bonus as the cost of the products can offset the processing cost to some extent. It is also a known fact that CO_2 conversion into fuel chemicals needs thermodynamic energy input apart from those required for overcoming the activation energy barrier. In fact, the high thermodynamic stability of CO_2 is responsible for its ability to store the external energy in the form of fuel chemicals synthesized out of it [1,65]. In fact, the energy spent for overcoming the activation energy barrier is a waste of energy; whereas, the energy spent for overcoming the thermodynamic energy barrier is energy storage. Thus, more amounts of thermodynamic energy requirement means more amount of energy storage in the form of chemical products formed in a particular endothermic reaction. That is the reason why always researchers look for the best catalytic systems to perform a particular reaction to occur *via* a path that is associated with the least activation energy barrier. Lower the activation energy barrier means lower the amount of energy wastage while driving that particular thermodynamically favorable reaction. The high thermodynamic stability of water ($\Delta E^\circ = -1.23$ V vs. NHE or 1.23 eV) is also responsible for its ability to store 1.23 eV energy in the form of H_2 and $\frac{1}{2}O_2$ gases formed in electrolysis of water. This same 1.23 eV equivalent electrical energy comes out again when these two gases are reacted in a fuel cell [1,10,12].

Even by replacing the usage of the *liquefied petroleum gas (LPG)* utilized for cooking with the electric stoves driven by electricity derived from sunlight, a significant amount of CO_2 gas generation can be avoided. Not only that now-a-days, even the cost of LPG gas has been increasing exorbitantly, and without the government aid or subsidy, it has become an unbearable cost for a common man living in India. In *Telangana* state of India, a 14.2 kg LPG gas cylinder costs about Rs. 1500/- without the Government subsidy, and with subsidy, it is about Rs. 950/- [66]. Even the petrol and diesel costs are being increased now-a-days in India very exorbitantly. If all the CO_2 gas generated at all its major outlets in India is converted into synthetic petrol using electricity derived from sunlight, and used in place of petrol and diesel utilized today to meet the energy requirements, there would be a lot of reduction in the importing of fossil fuels from foreign countries [1,39-46]. In fact, an inexpensive way of producing electricity from sunlight and using it for converting CO_2 gas produced at all its major outlets into fuel chemicals, and for splitting water into H_2 and O_2 gases can even change the global energy economy and energy dynamics of the world as well [1,18-22,24]. In view of the these and to solve the CO_2 associated global warming problem, at the outset, a simple, easy and highly economical method to produce electricity from sunlight is highly essential [10,12]. Furthermore, to continuously supply the intermittently available solar energy to the society without any back-up from fossil fuels, it is also required to be stored in a well usable form of energy. Fortunately, sunlight is abundant, clean, and free, and, all the world's population living areas also receive the required insolation levels (i.e., 150–300 watts/m^2 or 3.5–7.0 kWh/m^2 per day) [67]. With this insolation capacity, the required amount of electrical energy can be generated to meet all the needs of the society for buildings using a suitable sunlight to electricity generation technology.

1.2. The current status of electricity generating processes from sunlight

Preprints (www.preprints.org) | NOT PEER-REVIEWED | Posted: 15 November 2023 doi:10.20944/preprints202311.0965.v1

Today, there are four different types of methods available to generate electricity from sunlight. The first one is *Photovoltaics (PVs)*, which use p-n junctions formed out of a joining of p-type and n-type differently doped silicon semiconductor thin films, the binary III-V GaAs and InP systems, the *copper indium gallium selenide (CIGS)*, the *perovskite solar cells (PSCs)* based organic light absorbing chemical compounds such as, *methylammonium lead trihalide* (MLT) ($CH_3NH_3PbX_3$, where X is a halogen atom such as iodine, bromine or chlorine), with an optical band-gap between ~1.55 and 2.3 eV depending on halide content, etc., which can be amorphous, single or poly-crystalline in nature [1,22,68,69]. The second one is the *dye-sensitized solar-cells (DSSCs)* (or *Gratzel* cells) that use *cis-bis(isothiocyanato)bis(2,2'-bipyridyl-4,4'-dicarboxylato)ruthenium(II)*, (known as N_3 Dye), as a light capturing substance [70,71]. The third one is the *thermoelectric effect* (i.e., *Seebeck and Peltier modules*) that uses materials with suitable figure of merit such as, *bismuth telluride* (Bi_2Te_3) [72]. The fourth one is the *concentrated solar radiation* or *parabolic trough collectors* (PTC), which are typically operated at temperatures around 400°C [73].

In *parabolic trough collectors (PTC)* method, the heat energy captured is utilized by a heat engine (e.g., steam turbine) to produce electricity. The well-known examples of solar thermal power generation using PTCs are the *Solar Energy Generating Systems (SEGS)* in California, USA [74]. This particular system consists of nine power plants with a total capacity of about 354 megawatts (MW). However, the price of the electricity generated in this method has been found to be higher in comparison to the one obtained by burning fossil fuels at thermal power plants. The main reason for this high price of the electricity is the utilization of light concentrators, tracking of the light and distribution of electricity from far distances to the utility places. This PTC method has also been found to be quite cumbersome, and environmentally and ecologically danger particularly for the survival of the birds in those areas. Alternatively, low temperature solar thermal power generation, which operates using an *Organic Rankine Cycle (ORC)* offers an increasingly promising for domestic and smaller energy recovery installations when combined with *silicon photovoltaic cells (SPVC)* for waste-heat utilization. However, these systems are yet to be fully investigated for practical applications and to meet public energy needs.

The PVs based on CIGS [68], Perovskites, III-V GaAs and InP systems are either too expensive or not stable, and are still being developed in the laboratory. The existing PVs with high-quality III-V semiconductor stacks are associated with costly production steps and are found to be extremely expensive and hardly scalable. More affordable multi-junction PVs made with abundant materials (e.g., based on organic materials, Si, and/or perovskites) have not yet shown a significant increase in efficiency relative to the corresponding single-junction technology (i.e., SPVCs), which justifies the efforts in implementing the tandem architectures. Besides, the rigid design of the series-connected subcells has a current output limited by the lowest performing subcell, which further suffers from spectral mismatch losses at non-peak illumination hours or for different geographical locations. The main problem associated with the organic based *PSCs* is the stability, and they are yet to pass the required time period operation test in the real life conditions [69]. The most commonly studied perovskite absorber is *methylammonium lead trihalide* (MLT). Formamidinum lead trihalide ($H_2NCHNH_2PbX_3$) with band-gap energies between 1.48 and 2.2 eV was also found to be promising for this application. The minimum band-gap shall be closer to the optimal one for a single-junction cell than MLT so that it can exhibit higher efficiencies. The DSSCs suffer from the exorbitant price of the N_3 dye used in them, whereas, the efficiencies achieved so far in the thermoelectric modules is very low as materials with the required figure of merit are yet to be identified and/or developed [70,71].

1.3. Potential of silicon photovoltaic cell (SPVC) solar panels

It is a well-known fact that among various methods available today to generate electricity from sunlight, only the *SPVC* panels are the mostly deployed ones across the globe as a part of producing renewable electricity from sunlight, and are in the market for almost last 40 years [75]. In fact, electricity production from sunlight by following photovoltaic (PV) technology can be considered as a miracle. The SPVC panels provide significant social and environmental benefits as these panels do

Preprints (www.preprints.org) | NOT PEER-REVIEWED | Posted: 15 November 2023 doi:10.20944/preprints202311.0965.v1

not generate any greenhouse gases (GHGs). The SPVCs are also stand alone, and can be integrated, grid-connected and deployed in isolated locations. Furthermore, the semiconductor silicon used in these SPVC panels has an abundant raw material, which is non-toxic, relatively low-cost, allows the fabrication of cells with relatively high and stable sunlight-to-electricity (STE) conversion efficiency. It is also the most matured PV material, and has been a long-term market leader. In fact, the crystalline silicon (*c-Si*) technology is widespread and has deep skill and infrastructure not only for PV applications but also for the integrated circuit (IC) industries. The number of SPVC panels installed worldwide has grown exponentially since early 2000s, and it will be further grown during coming next few decades [1,4,76-82]. By the end of 2015, an estimated 222 gigawatts (GW) worth of SPVC panels have been installed worldwide. According to a recent report from the *International Renewable Energy Agency (IREA)*, USA, this number could reach to 4,500 GW by 2050. Furthermore, the production cost of SPVC panels has also been diminishing in the last decades, following a learning curve, which is now stagnating.

Although, almost 40 years back the SPVC panels have entered the market, and their manufacturing cost has also been came down to the lowest possible level, beyond which it is not possible to go down further, still almost all developed (excluding few countries including Germany, France, and Island) and still developing countries including India, meet more than 85% of their primary energy requirement from fossil fuels only. One the main reasons for this is could be as there is no affordable method to store the electricity derived from sunlight for that matter from any of the renewable energy resources, and to use it as and when required on the demand basis [1,18-22,24]. At present, the electricity produced from sunlight either needs to be utilized immediately or if it is a surplus one, then it is connected to a grid-system. During the peak hours (only 5-6 hours in a day), if electricity is produced to meet all the energy requirements of the society by using SPVC solar panels, then the electricity generated at thermal power plant is not needed. At that time, the thermal power plant is needed to be shut-down. As during remaining hours (i.e., for almost 19 hours) in a day, the sun is not available, at that time again those associated thermal power plants are required to be switched on. That everyday particularly during summer season switching on and off of thermal power plant has been found to be non-profitable venture in Germany and it incurred huge losses to those operators. Furthermore, the thermal power plants are designed to operate continuously not for intermittent operations.

1.4. Theoretical setbacks associated with SPVC solar panels

As with any renewable energy resource, the main limitation of SPVC solar panels is also the discontinuity between the solar radiation and power consumption during a day, year and geographical location. In addition to these, the theoretical maximum efficiency of a SPVC panel is <20%, and they convert >70% of the absorbed sunlight into the waste heat energy, which is dissipated into the atmosphere [83-88]. The various other limitations/setbacks associated with these SPVC panels are listed in Table 1 [1,89]. About 10% incident light is reflected back into the atmosphere from the front cover solar glass of SPVC solar panels. Up to about 8% of the incident light on SPVC panels is blocked by the grid and bus-bar lines printed on SPV cells. With a band-gap energy of about 1.1 eV, whose corresponding wavelength is ~1127 nm, the semiconducting Si material used in SPVC solar panels does not absorb sunlight reaching the earth surface with a wavelength range starting from 1127 nm to 2400 nm, which is accounted for about 30% of the sunlight reaching the earth surface. The percentage of sunlight reaching the earth surface with various wavelength ranges is given in Table 2 [1,89]. This sunlight energy data confirms that with 1.1 eV band-gap energy, the Si semiconductor in SPVC solar panels considers only around 70% of the sunlight reaching the earth surface for converting it into the electricity, and the remaining 30% incident sunlight is not absorbed or considered by these SPVC solar panels.

Table 1. Various limitations and setbacks associated with the commercial silicon photovoltaic cells (SPVC) panels [1].

S. No.	Limitation

 doi:10.20944/preprints202311.0965.v1

1.	The maximum achievable sunlight-to-electricity (STE) conversion efficiency is <20%. Hence, they need relatively larger land areas to get the desired voltage and power capacities.
2.	The light absorption is limited to only 70% of the sunlight reaching the earth surface as its band-gap energy is ~1.10 eV (i.e., with a corresponding wavelength of about 1127 nm). That means Si in SPVC panels does not absorb sunlight in the range of 1127 nm to 2400 nm, which is accounted for about 30% of the sunlight reaching the earth surface.
3.	About 10% incident light is reflected back into the atmosphere from the front cover solar glass itself.
4.	Up to about 8% of the incident light on SPVC panels is blocked by the grid and bus-bar lines printed on Si cells.
5.	Generates only DC current and conversion from DC to AC is an expensive process.
6.	The maximum voltage that can be achievable from SPV cell is only about 0.5 to 0.6 V.
7.	The STE conversion efficiency of SPVC panels decreases with the increasing operating (ambient) temperature at a rate of 0.5 V/°C or K.
8.	Creates considerable amount local heat island effect when deployed in large areas.
9.	They are not reusable and not-repairable, hence, the post retirement disposal is a big problem for SPVC panels as recovering materials from them has been found to be non-profitable venture.
10.	It requires direct irradiation of sunlight.
11.	It contains toxic heavy metals like Pb in the form of inter connectors used while joining several cells in series to achieve the desired voltage requirement.
12.	SPV cells are delicate and are easily damaged when accidentally hit by any small solid object.
13.	Relatively expensive as it involves highly complex and sophisticated equipment to fabricate SPVCs.
14.	Involves very expensive, highly toxic and pyrophoric liquid raw materials.

Table 2. Spectral distribution of Xe lamp (75 W, Hamamatsu, Japan) that generates the simulated solar light [1,89].

Region	UVC	UVB		UVA	visible						infrared						
Wavelength range	<250	250-280	280-320	320-350	350-400	400-450	450-500	500-550	550-600	600-650	650-700	700-800	800-900	900-1000	1100	1100-1500	1500-2000	2000-2400
Irradiance (%)	0.5	0.9	1.8	1.5	2.6	2.9	3.6	3.1	3.1	3.0	3.1	6.2	15.1	15.1	4.9	14.1	12.1	6.4

Apart from the above, the SPVC solar panels also suffer from several other limitations as summarized in Table 1 [1]. They are associated with high fabrication cost and cumbersome manufacturing procedure, hence, electricity generated by these SPVC solar panels is relatively expensive when compared with the one produced at thermal power plants by burning fossil fuels. They generate DC current instead of AC current as converting of DC into AC is also consumes some energy. The maximum voltage that can be generated by a single Si semiconductor cell in each SPVC solar panel is only about 0.5 to 0.6 V (Fig. 1) [1,90], and to obtain the required high voltage several of such single SPVCs needs to be connected in series, which generate considerable amounts of Ohmic loss. The sunlight-to-electricity (STE) conversion efficiency of SPVC solar panels decreases with the increasing operating (ambient) temperature at a rate of 0.5 V/°C or K (Fig. 2) [1,91,92]. They contain toxic heavy Sn-Pb solder metals coated over Cu stripe, which is used as grid and bus-bar lines, and as interconnecting wire to transport the generated electricity from one individual SPVC to other cell. The after use disposal is a great concern for SPVC solar panels, and the recycling of these panels has been found to be a no profitable venture. They create local heat island effect when deployed in large areas (Fig. 3) [1,93]. They are not reusable, recyclable, and are not physically very robust (i.e., they become redundant when they are accidentally hit with a physical object). Because of only <20% efficiency, SPVC panels need relatively large areas of land to generate the required amount of electricity [1,83-88]. Furthermore, when the operating temperature of SPVC panels is reached to a

Preprints (www.preprints.org) | NOT PEER-REVIEWED | Posted: 15 November 2023 doi:10.20944/preprints202311.0965.v1

certain higher level, which normally happens in peak summer period, they permanently and irreversibly lose their electricity generating capability [94]. The Qatari utility companies stopped using SPVC solar energy because the drop in the efficiency has been noted to be as high as 60%. Because of the combination of the latter country's extreme heat and dust accumulation on the solar panels, the fall in the efficiency has been noted to be up to 60%. In the case of SPVC solar panels, there's an irony in the fact that the locations best suited for solar energy generation are also limited by those same conditions in several central Asian countries such as, Saudi Arabia [95].

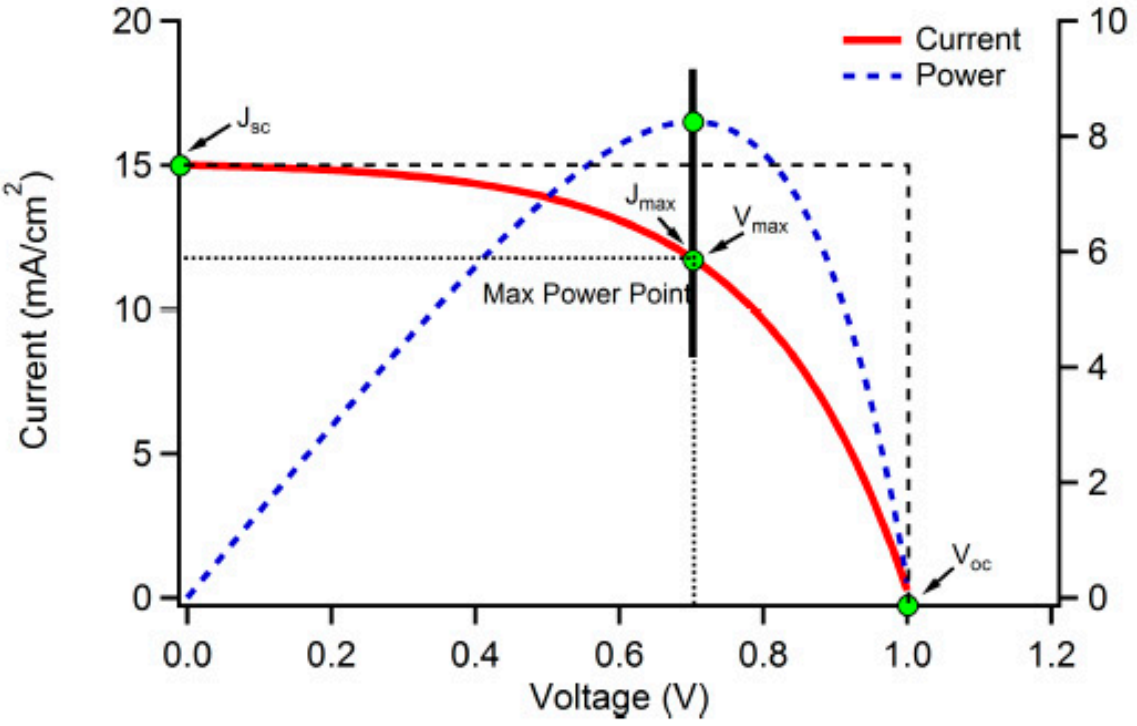

Figure 1. I-V and P-V characteristics of a silicon solar cell [1,90].

Preprints (www.preprints.org) | NOT PEER-REVIEWED | Posted: 15 November 2023 doi:10.20944/preprints202311.0965.v1

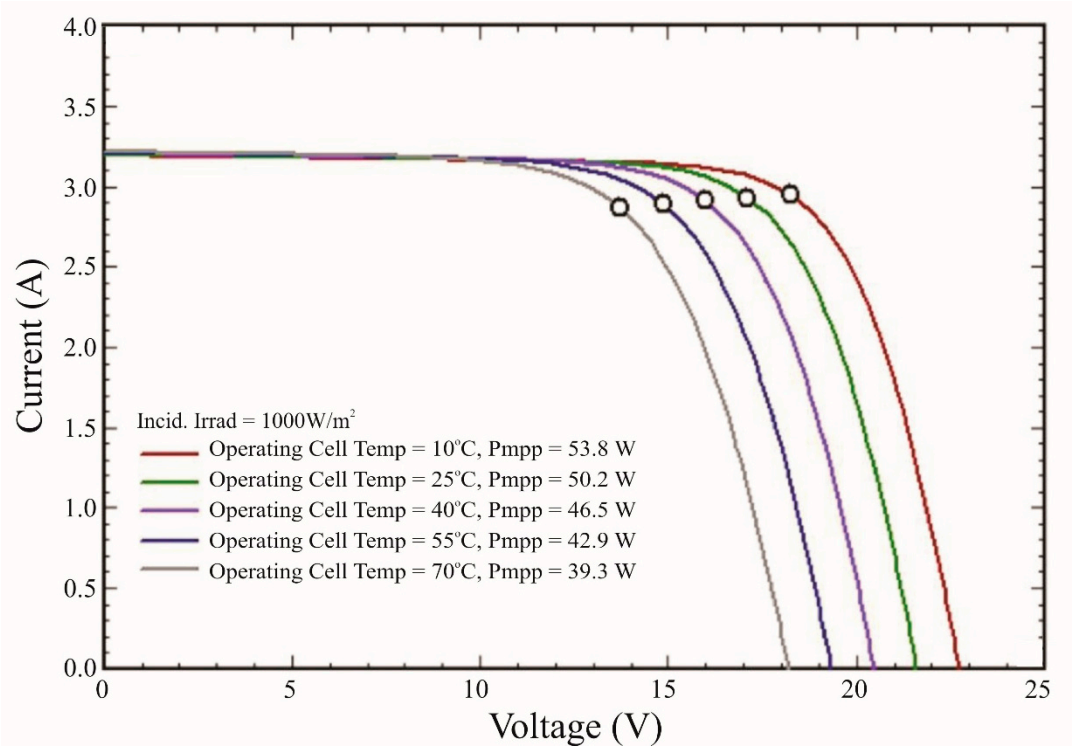

Figure 2. IV curves of a solar PV module under different operating temperatures [1,91,92].

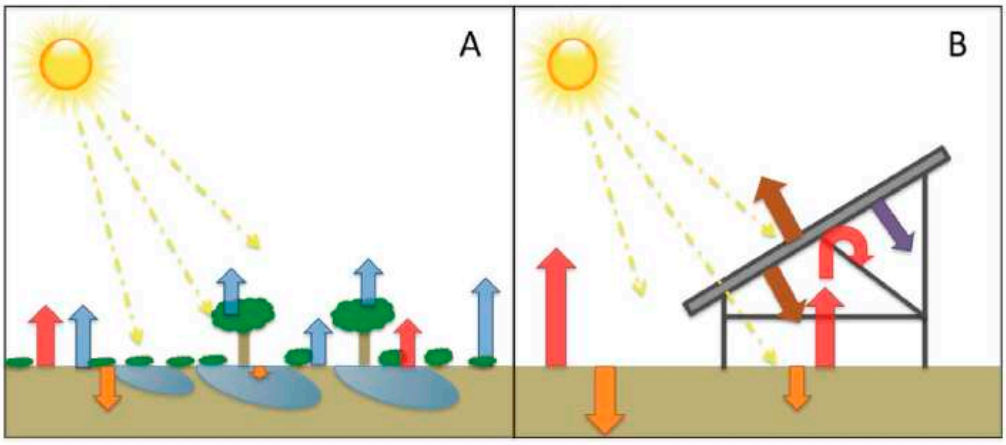

Figure 3. Illustration of midday energy exchange. Assuming equal rates of incoming energy from the sun, a transition from (A) a vegetated ecosystem to (B) a photovoltaic (PV) power plant installation will significantly alter the energy flux dynamics of the area. Within natural ecosystems, vegetation reduces heat capture and storage in soils (orange arrows), and infiltrated water and vegetation release heat-dissipating latent energy fluxes in the transition of water-to-water vapor to the atmosphere through evapotranspiration (blue arrows). These latent heat fluxes are dramatically reduced in typical PV installations, leading to greater sensible heat fluxes (red arrows). Energy re-radiation from PV panels (brown arrows) and energy transferred to electricity (purple arrows) are also shown [1,93].

Another major limitation of SPVC solar panels is that they are needed to be placed in a direction facing the south side with some angle of inclination so that while sun is travelling from east to west, it can strike the surface of these SPVC solar panels with the straight and direct light radiation. Similar to SPVC solar panels, the plant leaves also need sunlight to capture and store the solar energy in the form of food materials and bio-mass by using CO_2 and water as energy storing materials to feed the

Preprints (www.preprints.org) | NOT PEER-REVIEWED | Posted: 15 November 2023 doi:10.20944/preprints202311.0965.v1

human beings and animals [22]. However, a closer look at those plant leaves reveal that they do not face only south direction but all the directions to receive solar energy during the entire day. It has been found that the water (a liquid substance) present in the plant leaves is responsible for receiving the sunlight from all the directions and during the entire day time. Thus, the plant leaves suggest that the liquid containing surfaces receive more amount of sunlight from all directions without causing much of reflection back into the atmosphere [96]. It has also been established that the solid surfaces reflect more sunlight than those reflected by the liquid surfaces (Figs. 4 & 5) [1]. Furthermore, the SPVC panels also become quite hot during daytime [93].

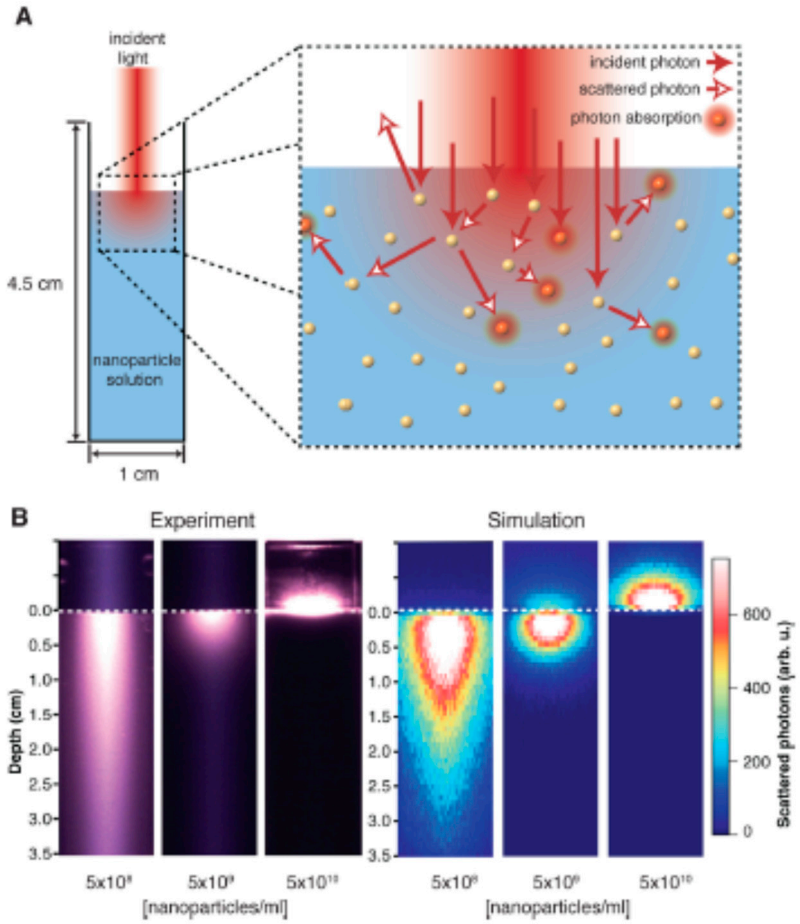

Figure 4. (A) Schematic illustrating characteristic experiment (left) where a dense solution of nanoparticles contained in a cuvette is illuminated with 808 nm laser light; multiparticle optical interactions in such nanofluids (right) where photons are scattered and/or absorbed. (B) Experimentally obtained (left) and Monte Carlo (MC) simulated (right) scattered light as viewed from the side of cuvettes containing nanoshell solutions of the indicated concentrations. Integration times are not the same for all three experiments [1,96].

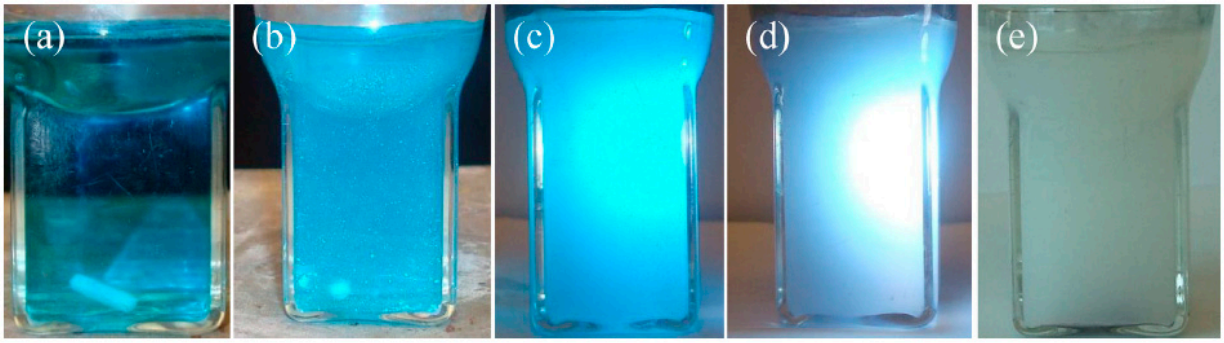

Preprints (www.preprints.org) | NOT PEER-REVIEWED | Posted: 15 November 2023 doi:10.20944/preprints202311.0965.v1

Figure 5. Digital photos showing decolourization of aqueous MB solution in the presence of TiO_2 nano-powder photocatalyst under the irradiation of a simulated solar light; (a) – pure aqueous 0.01 mM MB solution; (b) – aqueous 0.01 mM MB solution dispersed with TiO_2 nano-powder; (c & d) – aqueous 0.01 mM MB solution dispersed withTiO_2 nano-powder being irradiated with light having a wavelength range of (300–700 nm at 44 mW/cm^2 power density (rare & side views, respectively); & (e) slurry after exposing to the light irradiation. No light was detected backside of the reactor as the light passed into the reaction mixture solution was completely absorbed by the contents in it. Considerable amount of light reflection from the front face (wall) of the quartz-glass reactor can be seen from (d) photograph. The reflected light was determined to be about 6% [1,89].

In SPVCs, the *n*-type Si semiconductor doped with phosphorous and antimony (top layer) and *p*-type Si doped with boron (bottom layer) are deposited by following a *chemical vapor deposition (CVD)* technique to form a two layered thin film Si p-n junction cell with a band-gap energy of ~1.1 eV. Its top surface up to 8 to 10%, and the complete bottom surface are covered with an electrically conducting thin layer of Ag or Al to serve as grid and bus-bar lines, and as light reflecting bottom surface, respectively. In a one meter by two meters SPVC solar panel, 72 numbers of individual SPVCs are interconnected in a series using a copper thin stripe (coated with Sn-Pb layers to facilitate the soldering process while joining the individual cells together). Finally, these interconnected cells are placed in between two thin layers of ethylene vinyl acetate (EVA) sheets (5×10^{-4} m), which are in turn placed in between a top layer of fully tempered low-iron containing transparent solar glass (3.2 mm thick) sheet and a bottom polyurethane plastic (few mm thickness) sheet, and then all these parts are together hot compacted under vacuum so that no air-bubbles are trapped in the inter layers of the SPVC solar panel [67,88,97]. On the top surface of a SPVC, a very thin (about few hundred nanometer thick) layer of Si_3N_4 anti-reflection coating is given by following the same *CVD* technique. This latter layer also avoids to some extent the unforeseen oxidation of *c-Si* upon exposure to light irradiation in oxidizing environment, and to arrest the light reflection from SPVCs to some extent (Fig. 6) [1,98]. If SPVCs are not sealed in between two-EVA layers under vacuum properly, Si undergoes oxidation into SiO_2 with a band-gap energy of ~9.0 eV upon irradiation with sunlight in presence of air/moisture atmosphere. Once Si is converted into SiO_2, it loses its ability to capture sunlight and to turn it into electricity or heat energy as the sunlight reaching the SPVC solar panel do not possess the band-gap energy higher than 3.2 eV. The sunlight with 3.2 eV energy cannot excite the *valance-band (VB)* (i.e., the *highest occupied molecular orbital (HOMO)* electrons of SiO_2 into its *conduction band (CB)* (i.e., into the *lowest unoccupied molecular orbital (LUMO)*) as its band-gap energy is ~9.0 eV to create the electron-hole pairs. When Si undergoes ionization upon irradiation with sunlight (i.e., light with <1125 nm wavelength) having energy higher than that of its band-gap (i.e., 1.1 eV) by exciting its VB electrons into CB, there is a creation of electron-hole pairs with definite oxidation and reduction potentials [80]. These Si oxidation potentials can pull electrons from water molecule when it comes into contact with the ionized Si^{4+} ions and oxidizes it to form O_2 and H_2 gases. Furthermore, if any air or moisture is present between the EVA layer and SPVC after hot-compaction into SPVC solar panel, the entrapped air/moisture undergoes volumetric expansion when it receives the heat generated by *c-Si* cells and creates considerable amount of strain capable of breaking the very-thin and highly brittle *c-Si* cells. Thus it can cause a very serious damage to the SPVC cells and decreases the overall STE generating efficiency of these solar panels. The thin Si_3N_4 layer present on *c-Si* cells cannot confer sufficient strength to withstand the strain and to prevent SPVCs from breakage. Furthermore, when the amount of heat dissipated by EVA, glass-sheet, and polyurethane bottom protective plastic sheet, and by thin strips of electrically conducting Sn-Pb coated Cu interconnecting material printed on top and bottom surfaces of SPVCs not enough, the generated heat can also cause the irreversible loss of electricity generating ability of p-n junctions of these SPVCs. Fortunately, in most locations, solar panels are operated within the comfortable temperature range; hence, not much efficiency is lost as there is the decrease of only 0.5 V per every degree temperature rise [80]. Furthermore, the voltage generation is inversely proportional to the current generating ability of *c-Si*, which increases with the increase of operating temperature.

Preprints (www.preprints.org) | NOT PEER-REVIEWED | Posted: 15 November 2023 doi:10.20944/preprints202311.0965.v1

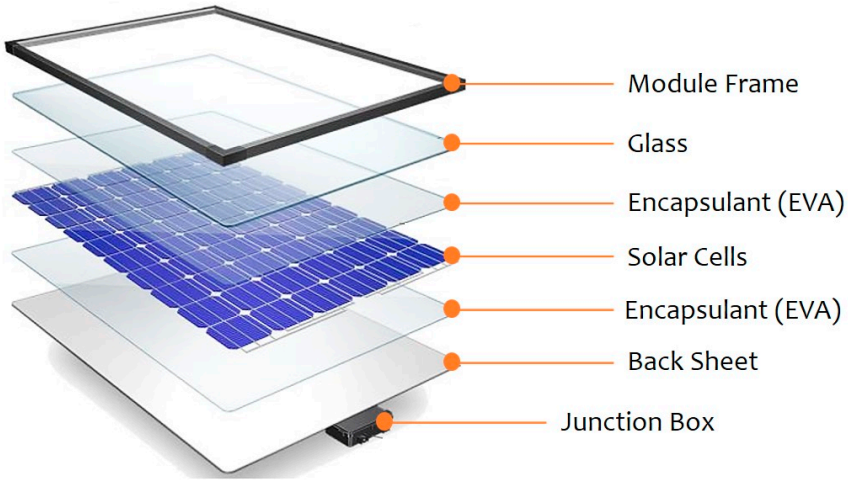

Figure 6. Silicon photovoltaic cell (SPVC) solar panel components [1,98].

In order to have the continuous performance of SPVC solar panels even after exposure to the increased temperatures, their laminating materials have to withstand 85°C in thermal cycling and damp heat tests according to the *International Electrotechnical Commission (IEC)* 61215 [99]. So far several efforts were made to reduce the operating temperature of SPVC solar panels, and as a part of these developments, *photovoltaic thermal (PV/T)* systems have been introduced to increase the STE conversion efficiency as they take off the *in situ* generated heat energy from the SPVC solar panels by a coolant liquid (mostly water), and thus collected heat energy in the form of hot-water is utilized for house-hold applications [1,81,91,92,96,100-108]. Apart from SPVCs, other semiconducting materials were also investigated for collecting solar energy in the form of heat energy for hot-water applications (a Japanese patent - JP2016145653). In PV/T systems, the heat carrying working fluid (WF) is not directly coming into contact with the heat generating SPVCs. Furthermore, in these latter systems, the SPVCs and the WF are separated by either EVA layer or by heat absorbing metal sheet followed by Cu tube. Besides that in order to avoid the oxidation of Si in SPVCs, they do not allow coming directly in contact with the WF. In fact, when the light energy absorbing SPVCs are fully immersed in a liquid solution, the *in situ* generated heat energy is absorbed by the liquid immediately and there will not be any associated heat losses during the transmission from one material to the another material. The thermal conductance of the layer between SPVCs and the metal plate used in the PV/T systems can be determined using Eq. (1) [109].

$$h_{pv\text{-}metal} = [(t_{EVA})/(k_{EVA})]^{-1} \quad (1)$$

The specific conductivity of an EVA layer used in SPVC solar panels to protect the semiconducting Si from oxidation is k_{EVA} = 0.35 W/m.K, and the thickness EVA lamination layer (t_{EVA}) commonly used is 5×10^{-4} m. This corresponds to a thermal conductance ($h_{PV\text{-}metal}$) of about 700 W/m².K [81]. Stagnation, although infrequent, is a possible occurrence in forced circulated solar PV/T thermal systems [1,92,107,108], and is caused by low thermal demand (fully charged thermal storage tank), power outages (no electricity available to run the pumps) and other problems leading to a no-flow condition (plugged pipes, leaks, broken pumps, etc.). In these situations, the collector temperatures only depend on the idle heat losses and on the insolation heat dissipating capability. *Consequently, stagnation temperatures sometimes reach up to 220-350ºC for evacuated tube collectors, 170-210ºC for flat-plate collectors with selective absorbers and 115-150ºC for flat-plate collectors with non-selective absorbers* [77]. Although, the SPVCs can withstand temperatures up to 220ºC, the EVA encapsulate loses its mechanical properties at 130-140ºC and undergo delamination [1,77]. The occurrence of such high collector temperatures can cause the accelerated ageing of temperature sensitive components leading to their eventual failure, safety hazards for humans, uncomfortable acoustic emissions due to condensation pressure shocks (measured up to a maximum pressure of 6 bar for 60% water + 40% propylene glycol solution), enhanced vulnerability to hot spots resulting from manufacturing

 doi:10.20944/preprints202311.0965.v1

imperfections and the vaporization of common heat carrier fluids, and their potential release into the atmosphere from the loop *via* safety valves. Owing to these problems, although the overall STE conversion efficiency of PV/T systems has been found to be higher than those of pure SPVC solar panels, their usage has been very limited. Nevertheless, the components used in the fabrication of SPVC solar panels such as low iron containing top solar glass, and the EVA polymer layer ensure that maximum amount of *in situ* generated heat energy is dissipated as soon as possible, which is the reason behind the normally absorbed local heat island effect when a large number of SPVC solar panels are deployed [80]. Furthermore, the SPVC solar panels also get detached in very windy conditions, and consequently can cause damage to property and persons. In addition to these technological limitations, another disadvantage of SPVC solar panels is it is often required to get the permission of the planning commission in certain jurisdictions in order to install SPVC solar panels as they can have a visual impact in areas where architectural integrity is required.

1.5. The environmental concerns of the retired SPVC solar panels

It is a known fact that the SPVC solar panels do not generate power forever. The industry standard life span of these solar panels is about 25 to 30 years, and the panels installed at the early end of the current boom (i.e., at the beginning of 1990s) are not long from being retired. For each and every passing year, more and more panels will be retired from the service; it will soon start adding up to millions, and then tens of millions of metric tons of material. According to a recent survey, by the end of the year 2020 in Japan, the solar panel waste will exceed 10,000 tons, it will reach 1,00,000 tons by 2031, it will be reaching 3,00,000 tons by 2034, and between 2034 and 2040, it will be between 7,00,000 to 8,00,000 tons annually [1,110]. The projected 8 lakh tons is equivalent to 40.5 million panels. To dispose of that amount in a year would mean getting rid of 1,10,000 panels per day. In response to this waste management, *M/s. Toshiba Environmental Solutions, Japan*, says that recycling of SPVC solar panels do not provide any profit as the expenditure incurred for recycling process is higher than the cost of the materials recovered from the recycled SPVC solar panels [110]. Furthermore, the current price of these solar panels in the market is considered to be below their manufacturing cost, and consequently, are unsustainable, in large part because several leading non-Chinese firms in the industry have recently announced losses cutbacks or massive write-downs or filed for bankruptcy. Furthermore, a new study by Environmental Progress warns that the toxic waste generated from used SPVC solar panels pose a global environmental threat [111]. A Berkeley-based group found that SPVC solar panels create 300 times more toxic waste per unit of energy generated when compared with the one exhibited nuclear-power plants. Discarded SPVC solar panels, which contain dangerous elements such as lead, chromium, and cadmium, are piling up around the world, and no techniques found so far to mitigate their potential danger to the environment [111]. A lot is talked about the dangers of nuclear waste, but that nuclear waste can be carefully monitored, regulated, and disposed of. But there is no idea about an enormous amount of SPVC panels that could cause so much ecological damage. SPVC solar panels are considered a form of toxic, hazardous electronic or "e-waste". The e-waste is burned in order to salvage the valuable copper wires for resale. Since, this process requires burning off EVA and polyurethane plastics, the resulting smoke contains toxic fumes that are carcinogenic and teratogenic (birth defect-causing) when inhaled [111].

In fact, today, the cost of SPPV solar panel installations is dominated by packaging and systems integration, which are fixed costs [22]. These trends indicate that reducing the SPVC solar panels manufacturing cost is no longer sufficient to improve its competitiveness. Furthermore, manufacturing of SPVC solar panels can also have consequences for workers and for environment throughout their life cycle (from raw material extraction and procurement to manufacturing, disposal, and/or recycling) [1,112]. Since, the SPVCs manufacturing has roots in the electronics industry, many of the chemicals found in e-waste are also found in SPVCs, including Pb, Br flame retardants, Cd, and Cr. The manufacturing of SPVCs involves several toxic, flammable and explosive chemicals. Many of those components suppose a health hazard to workers involved in the

 doi:10.20944/preprints202311.0965.v1

manufacturing of these SPVC solar panels [113]. Today, the disposal of electronic products has been found to be an escalating environmental and health problem in many countries.

1.6. Is it possible to fully depend on SPVC solar panels to meet all the energy needs of the society without any backup from fossil fuels?

The major economic failure of SPVC solar panels can be seen from the Germany's *Energiewende* program [1,114-116]. The main achievement of *Energiewende* program has been the increase of renewable energy from solar, wind and biomass in the overall consumed electricity from 3.4 % in the 1990s to almost 40 % today in the Germany. It can be appreciated that *Energiewende* program successful in making everybody a part of this program by installing their own renewable energy generating systems. This really made up the success of the energy transformation and brought acceptance that people are relying on it [1]. However, the first failure of this program has been the requirement of the massive government subsidies from taxpayers' money to operate, and the Germany accelerated the program without much of planning, so it is no surprise that $100 billion was wasted on the installation of roof top solar panels [1,116]. In fact, the two major objectives of Germany's *Energiewende* program are complete elimination of nuclear energy usage and complete minimization of CO_2 release into the atmosphere [1]. However, none of these two objectives were completely met [1]. The major obstacle for not achieving these objectives is due to the fact that the sun does not shine in the winter so the most solar energy is generated when the least electricity is needed period that is summer. Often it is thought that impressive amounts of solar energy being generated and used in the country, but those figures come from the summer season. In the case of wind, it is usually a daily stat taken when the wind was blowing strongest that day. In reality, only about 10% of energy throughout the year is renewable [1]. The next failure is that wind and solar power are intermittent – the sun does not shine always and the wind does not blow always [1]. Renewable energy gets access to the grid when it is available, essentially pushing thermal energy from coal offline. Thermal plants are designed to run all day, every day and now they are only marginally profitable because this energy is still required when intermittent solar and wind energy are not available. The main reason for its failure is due to the non-availability of the facilities to store the surplus electricity generated during summer period. About 60% of electricity is still produced by burning coal and natural gas, which are imported fossil fuels from other countries. As there is also no viable storage mechanism for wind and solar energies – it has to be used when it is produced. That means back-up is required, which in Germany's case is the coal**.** The country started the *Energiewende* program with a goal to eliminate the nuclear energy by the year 2000, which provides as much as 25 per cent of power. As a result of phasing out nuclear energy and due to the using of coal as the back-up for renewables, GHGs have risen in the country, exactly the opposite of what they implemented the energy program to do [1]. There is a reason only 2 per cent of global energy is produced today by solar and wind together – they are not viable. They are intermittent sources that cannot be stored. Furthermore, it takes a lot of work to concentrate these types of energies for actual usage. Until humans find a way to capture and store solar and wind energies to be used in a free standing facility without back-up, renewable energy plans are just an expensive and faulty government experiments funded by the public [1,114-116].

In view of the above, to build a society fully supplied by the vast but intermittently available solar energy, it is also required to develop a practical self-sustainable energy package capable of directly supplying a dispatchable and most usable form of energy vector to the society. For this purpose, the successful development of both the inexpensive, highly efficient, and highly stable STE production method, and effective *AP* process are needed [1,18-22,24,25]. It is known that the electrochemical conversion of CO_2 into fuel chemicals requires voltages in the range of 2-3 V to overcome the thermodynamic energy requirements together with the activation energy barriers. So, with conventional SPVC solar panels, at least 5 series-connected SPVCs are required to drive such reactions, which imply significant Ohmic and current mismatch losses in the cells' interconnections. In view of these, it is difficult to completely depend on expensive SPVC solar panels for renewable

 doi:10.20944/preprints202311.0965.v1

energy production. Hence, another inexpensive, simple, and easy to fabricate technology to generate electricity from sunlight is needed to be developed with commercial viability [1].

1.7. Semiconductor assisted photothermal effect (SAPE)

It is a known fact that all the semiconducting materials including Si (amorphous, single- and poly-crystalline), TiO_2, MgB_2, ZnO, FeO, Fe_2O_3, Fe_3O_4, Co_2O_3, Co_3O_4, Cu_2O, NiO, WO_3, CdS, PbS, PbSe, PbTe, PbS, InN, Ge, GeSb, SiC, Si_3N_4, InSb, InAs, GaP, GaSb, GaAs, GaN, CIGS, cadmium telluride, copper indium sulphide, etc., either in pure form or after doping them with any other single metal or non-metal or a combination of elements in elemental form or in compound form, and all organic dye materials (including those employed so far in all the dye-sensitized solar cells (DSSCs) and Perovskite solar cells (PSCs)), and low energy band-gap polymers absorb light energy upon their exposure to the sunlight [1]. Semiconducting materials upon exposure to light energy higher than that of their band-gap energy excite their valance band (VB) (i.e., HOMO) electrons into their corresponding conduction band (CB) (i.e., into LUMO), and create holes having positive charge in their in the VB orbitals. When the excited electrons are recombined again with their corresponding hole-vacancies in the VB owing to their equal and opposite charges, the absorbed energy is released back again as light energy, which is manifested in the form of photoluminescence (PL). The released light energy is quantized and is the characteristic signal of that semiconducting material. The PL is two types, i) fluorescence and ii) phosphorescence. The kind of PL generation is decided by the type of band-gap (direct or indirect) present in that particular semiconducting material. In fact, in SPVC solar panels with *p-n* junctions generate electricity upon irradiation with sunlight that cause excitation of electrons from VB to CB of *c-Si* semiconducting material. However, when the semiconducting materials are irradiated with light energy much higher than that of the band-gap energy (for example Si having a band-gap energy of 1.1 eV is irradiated with 3.0 eV light), then light energy equivalent to its band-gap energy is converted into the PL or electricity generation in SPVC solar panel, and the remaining excess energy (for example 1.9 eV = 3.0 eV – 1.1 eV) is converted into the heat energy [1,117]. It is also a known fact that every photon (E = hν) causes excitation of only one electron from the valance orbital of a Si atom. Furthermore, when the SPVC solar panels are operated under the open-circuit (OC) voltage and short-circuit (SC) current conditions, the complete light energy absorbed by SPVCs is converted into only heat energy without generating any electricity [1,76,88,97,118,119]. In such OC voltage and SC current conditions, about >90% of the incident light gets converted into heat energy by SPVC solar panels. The process of heat generation by a semiconducting material upon exposure to a light energy is referred to as the "*Semiconductor Assisted Photothermal Effect (SAPE)*" [1].

The SAPE is also responsible for generating well-known sensitive spectral information in methods such as, *thermal lensing (TL)*, *photoacoustic spectroscopy (PAS)*, and *photothermal deflection spectroscopy (PDS)* [1,120]. Furthermore, the SAPE can also be correlated very well with the heat generation by the resistive heating elements upon supplying with a suitable electrical energy, and with the heat generated by the electrodes used in electrochemical reactions. The resistive heating elements such as, $MoSi_2$, graphite, zirconia with fluorite structure, nichrome (nichrome 80/20; 80% nickel, 20% chromium), Kanthal (a trademark for a family of iron-chromium-aluminium, FeCrAl) alloys, Cupronickel (copper-nickel, CuNi, is an alloy of copper that contains nickel and strengthening elements, such as iron and manganese), etc., convert electrical energy into heat energy according to the *Joule's law* ($W = I^2R$) [1,121]. Similarly, for example, when water is electrolyzed in 30 wt.% aqueous KOH solution by immersing an anode made of Ni or stainless steel (SS), and a cathode made of Ni connected to a 12 V or 16 V battery (*DC current*), out of which only 2 V energy is consumed for splitting of water into H_2 and O_2 gases, and the remaining 10 V or 14 V is consumed in the generation of heat by those electrodes resulting into the generation of steam instead of H_2 and O_2 gases. To avoid the generation of steam in the electrolyzers that use 12 V or 16 V DC batteries, the concept of using electrolyzer stack has been introduced [1,122]. The stacks in both alkaline or *PEM (polymer or proton exchange membrane)* electrolyzers ensure supply of only 2 V electricity between any two adjacent electrodes, which act as anode and cathode, by introducing suitable number of neutral (bipolar) plates between the end plates of anode and cathode connected to a battery. When 16 V

Preprints (www.preprints.org) | NOT PEER-REVIEWED | Posted: 15 November 2023 doi:10.20944/preprints202311.0965.v1

battery is connected, then seven (7) neutral plates are placed between anode and cathode connected to the battery terminals so that there will be total eight (8) pairs of anodes and cathodes (i.e., cells); where each pair can draw only 2 V electricity from the battery. Based on these findings, it can be concluded that when certain semiconductor materials are supplied with energy not bearable by them, they generate heat energy.

In a recent patented process, a method and a device were employed to turn sunlight into heat energy (A Japanese patent - JP2016145653) [1]. This device consists of a metallic tube through which the heat carrying working fluid (WF) is flown. The STE generating materials coating given on metallic tube consists of a STE conversion layer made of manganese silicide sandwiched in between two layers of infrared reflecting material (i.e., between metallic tube and manganese silicide) and a antireflection material coating on top of the manganese silicide. In this method, the heat generating material, i.e., manganese silicide, does not directly come into contact with the heat carrying working fluid, which flows inside the metal copper tube, whereas, the layers of the light absorbing materials are given on the outer surface of the metallic copper tube. The drawback of this method and device is the low STE generating efficiency [1].

1.8. Nanoparticle assisted photothermal effect (NAPE)

The irradiation of non-semiconducting nanoparticles such as, noble metal nanoparticles, metal oxides, carbon nanosystems, etc., after suspending them in certain liquids such as, water with suitable light energy was found to result in the generation of heat energy within that solvent. This latter process is referred to as the "*Nonoparticle Assisted Photothermal Effect (NAPE)*" [1,96]. Irrespective of the material type, whether it is an insulator (e.g., SiO_2), semiconductor (e.g., TiO_2, and *c-Si*), or conductor (e.g., Au and Ag), when nanoparticles of these materials are immersed in a solvent, and exposed to the suitable light energy, they generate heat energy by absorbing the light energy within that solvent. Among the various nanoparticles investigated so far, the gold (Au) nanoparticles have been found to be more promising to convert light energy into heat energy with highest conversion efficiencies and stability [1,96]. When one dimensional Au nanoparticles or nanorods are immersed in an aqueous medium and exposed to a near-infrared light energy, the photon-to-thermal (PTT) energy conversion was noted [123,124]. Even though, the Au nanoparticles are widely used in photothermal applications, they face certain serious challenges: due to weak metal–metal bonding, they undergo Coulomb explosion, resulting in aggregation, fragmentation or melting. The stability of the nanoparticles in dispersions also depends on the robustness of the surfactants and ligands involved. Nevertheless, the relationship between the noble metal nanoparticles and amount of heat energy generation upon irradiation with a particular amount of light energy is yet to be understood and established the theoretical basis for it [1,125]. The factors that decide light-to-heat generation *via* NAPE include: i) substantial broadband light absorption out of sunlight reaching the earth surface, ii) extremely low PL quantum yield, and iii) stability of the material in the given operating conditions.

Recently, a polycrystalline bulk magnesium diboride (MgB_2) powder was also investigated as a photothermal material and found that it is indeed a broadband light absorbing material with weak PL and excellent photo-stability in the solid-state powder form. The heat-flow from MgB_2 was registered with an ultrahigh value of 45 W/g upon irradiation with a low-pressure mercury vapor lamp (wavelength: 250–450 nm; irradiance: 800 mW/cm^2) with a photo-to-thermal energy conversion efficiency of about 83% (with an error of about 1.86%) [1,125]. In order to realize a practical model, the light-induced heat generated by MgB_2 was also investigated by generating electricity using a thermoelectric generator (TEG) (open circuit voltage: 125 mV is when illuminated by a solar simulator). The bulk MgB_2 powder was also found to be a photo-stable material under different irradiation conditions, and the photothermal effect was found to be highly reproducible [1,125]. However, the light-to-electricity conversion efficiencies recorded in all these so far reported methods have been found to be very meager and not suitable for industrial applications.

1.9. Semiconductor and liquid assisted photothermal effect (SLAPE)

Preprints (www.preprints.org) | NOT PEER-REVIEWED | Posted: 15 November 2023 doi:10.20944/preprints202311.0965.v1

Since, neither the SPVC solar panels, nor SAPE or NAPE phenomenon absorb the complete sunlight reaching the earth surface to convert it into electricity, it is required to have a new method or system to completely absorb the sunlight reaching the earth surface in the wavelength range of about 250 nm and 2400 nm, of course, with varying intensity [1]. It is known that silicon semiconductor absorbs light having wavelength <1127 nm, whereas, the liquid solutions absorb infrared radiation from 1100 nm to 2400 nm. To capture the complete sunlight reaching the earth surface, for the first time, the SLAPE concept was employed in this investigation to generate initially heat energy from sunlight, and then electricity from that *in situ* generated heat energy with the help of an electric generator and the reciprocally moved steam engine [1,126]. When semiconducting materials including *Si (amorphous, single- or poly-crystalline)*, black silicon wafers, etc., are suspended in electrochemically quite stable organic solvents such as, γ-butyrolactone (γ-BL), γ-valerolactone (GVL), methoxyacetonitrile (MAN), acetonitrile (AN), trimethyl phosphate (TMP), propylene carbonate (PC), 1,2-butylene carbonate (BC), 3-methoxypropionitrile (MPN), etc., which are referred to as non-working fluid (NWF), and exposed to the sunlight, none of the semiconducting materials identified so far can either oxidize or reduce these NWFs as their oxidation and reduction potentials are much higher than those of the semiconducting materials (Table 3) [1,127-129]. Thus, the required characteristics of these NWFs should be i) a very high electrochemical stability window of about 7 V, ii) high-boiling point (up to 200°C), and iii) fully dried solvents without the presence of any trace of moisture. If water is present in these NWFs, when semiconducting materials suspended in them are exposed to sunlight, they undergo oxidation. Except, pure TiO_2, and ZnO, all other semiconducting materials lose their light absorbing capabilities when they are exposed to sunlight in the presence of water as water undergoes oxidation into H_2 and ½ O_2 gases [1]. Not only water, if any other organic solvent or matter with lower oxidation and reduction potentials is exposed to sunlight together with any of the semiconducting material, those organic matter undergo oxidation into CO_2 and to other stable molecules, which is nothing but a photocatalytic reaction. This process can be clearly seen from the contents of Fig. 5 [1,89], where the methylene blue organic dye completely underwent de-colorization or decomposed in the presence of B-doped TiO_2 and water upon exposure to a light energy. The heat-energy generated from sunlight can be used to boil a low-boiling-temperature solvent such as, dichloromethane (DCM), hydro-fluoro-ethers (HFEs) including HFE-7000 and HFE7100, etc., as working fluids (WF) to generate enough pressure in them to rotate the electric generator (dynamo) connected to a reciprocally moved steam engine (RSE) that turns heat-energy into rotational mechanical to generate both AC or DC electricity [1]. The major required characteristics for WFs are i) a low-boiling point, ii) higher latent heat of vaporization, iii) higher density and higher molecular weight than those of water along with iv) non-flammable and v) non-corrosive characteristics. Furthermore, they should be compatible with stainless steel, copper, aluminum, polypropylene, polyethylene and nylon. In addition to these, it shall be a dry fluid with a positively slopped saturation vapor curve so that it can be in a dry vapor state when it is in the steam engine and shall not contain any liquid droplets, otherwise, those liquid droplets can damage the moving parts within the system having the capability to turn the heat energy into a mechanical energy. If a wet (negatively slopped saturation vapor curve) WF is used, it would be needed to be superheated before pumping it into such system. The WFs shall also be environmentally friendly and possess zero ozone depletion potential (ODP), and they should not cause any threat to the human health or to the environment [1,130].

Table 3. Electrochemically stable organic solvents that can be employed as non-working fluids (NWFs) in SLAPE solar panels [1,127-129].

Solvent	T_f[a] (°C)	T_b[b] (°C)	d[c] (g/cm³)	[d] (mPa.s)	ε_r[e]	LD_{50}[f] (g_{oral} kg_{rat}^{-1})	P^*[g] (kPa)	E_{red}[h] (V vs. SHE)	E_{oxi}[i] (V vs. SHE)	ECW[j] (V)
N,N-Dimehylacetamide (DMAc)	20	166	0.94	0.93	37.8	5.68	9.77	-	-	-

Preprints (www.preprints.org) | NOT PEER-REVIEWED | Posted: 15 November 2023 doi:10.20944/preprints202311.0965.v1

N-Methyl-2-pyrrolidone (NMP)	24	204	1.03	1.70	32.2	3.91	0.84	-	-	-
Nitromethane (NM)	29	101	1.13	0.61	36.7	0.94	4.88	1.0	2.9	3.9
γ-Valerolactone (GVL)	31	208	1.05	2.00	42.0	8.80	0.027	2.8	5.4	8.2
Methoxyacetonitrile (MAN)	35	120	0.96	0.70	36.0	0.98	2.50	2.5	3.2	5.7
γ-Butyrolactone (γ-BL)	43	204	1.13	1.73	39.1	1.54	0.43	2.8	5.4	8.2
Acetonitrile (AN)	44	82	0.79	0.34	35.9	6.69	11.81	2.6	3.5	6.1
Trimethyl phosphate (TMP)	46	197	1.07	2.20	21.0	0.84	0.13	2.7	3.7	6.4
Propylene carbonate (PC)	49	242	1.20	2.53	64.9	5.00	0.017	2.8	3.8	6.6
1,2-Butylene carbonate (BC)	53	240	1.14	3.20	53.0	5.00	0.0056	2.8	4.4	7.2
3-Methoxypropionitrile (MPN)	57	165	0.94	1.10	36.0	4.39	0.28	2.5	3.3	5.8
N,N-Dimethylformamide (DMF)	60	153	0.94	0.92	36.7	2.80	0.49	-	-	-
Diglyme	64	160	0.94	0.99	7.23	5.40	0.45	-	-	-
1,2-Dimethoxyethane (DME)	69	85	0.86	0.46	7.20	5.37	6.38	-	-	-
4-Methyl-2-pentanone	84	117	0.80	0.55	13.1	2.08	2.50	-	-	-
Ethyl acetate (EA)	84	77	0.89	0.43	6.02	5.62	12.57	-	-	-
2-Propanol	88	82	0.78	2.04	19.9	5.05	5.76	-	-	-
Nitroethane (NE)	90	115	1.05	0.68	28.0	1.10	2.08	1.1	3.2	4.5
Toluene	95	111	0.86	0.55	2.38	5.58	3.79	-	-	-
Hexane	95	69	0.65	0.29	1.88	25.0	20.12	-	-	-
Acetone	95	56	0.78	0.30	20.6	5.80	30.72	-	-	-
Dichloromethane (DCM)	95	40	1.32	0.39	8.93	2.00	57.99	-	-	-
Methanol (MeOH)	98	65	0.79	0.55	32.7	1.98	16.89	-	-	-
Tetrahydrofuran (THF)	108	66	0.89	0.46	7.58	2.45	21.55	-	-	-
Ethanol (EtOH)	115	78	0.78	1.08	24.6	10.47	7.85	-	-	-
1-Propanol	126	97	0.80	1.94	20.5	8.04	2.79	-	-	-

[a] T_f: freezing point of pure solvent [128]. [b] T_b: boiling point of pure solvent [128]. [c] d: density [128]. [d] μ: viscosity [128]. [e] ε_r: relative permittivity [128]. [f] LD_{50}: median lethal dose (50%) data from materials safety data sheets of Sigma-Aldrich [127]. [g] P^*: saturated vapor pressure at room temperature [128]. E_{red}: limiting reduction potential & [i] E_{oxi}: limiting oxidation potential (0.65 M Et_4NBF_4, 25°C, glassy carbon, 5 mV s^{-1}, and 1 mA cm^{-2} as threshold) [129]. The potential is converted by SCE = 0.24 V vs. SHE. ECW: electrochemical window (ECW = $E_{oxi} - E_{red}$).

In SLAPE, the semiconducting materials in conjunction with an electrochemically stable organic solvent (NWF) such as, γ-butyrolactone are employed to capture the complete sunlight reaching the earth surface (infrared portion of the sunlight is captured by the γ-butyrolactone and the remaining portion of the sunlight) is captured by the semiconducting material such as Si in SPVCs and black silicon wafers, when they are together exposed to the sunlight [1]. This latter method of capturing sunlight by semiconducting material in conjunction with organic solvent is referred to as the "SLAPE". When the semiconducting materials of either inorganic or organic type with band-gap energies in the range of 0.5-3.2 eV are fully immersed in γ-butyrolactone and exposed to the sunlight,

Preprints (www.preprints.org) | NOT PEER-REVIEWED | Posted: 15 November 2023 doi:10.20944/preprints202311.0965.v1

they can together absorb more than >80% of the sunlight falling on them. If the semiconducting particles are suspended in γ-butyrolactone are exposed to the sunlight, they can absorb the maximum light energy as they can be packed with 100% packing factor like liquid crystal display (LCD) screen. In such a case, all the three concepts viz.: SLAPE, NAPE and SAPE are operative together in synchronization [1]. In order to realize such a combined effect to capture the sunlight to generate heat-energy, in this study, the multicrystalline SPVCs in conjunction with γ-butyrolactone as non-working fluid (NWF) were employed to capture the sunlight and to generate heat energy to boil DCM working fluid (WF) present in a copper tube conduit. Thus *in situ* generated heat-energy from the captured sunlight upon exposure of the SLAPE solar panels fabricated in this study was converted into electricity using custom made electric generator and commercially available laboratory scale reciprocally moved steam engine [1]. Thus obtained results obtained in these experiments are presented and discussed in this article.

1.10. Transpiration

As liquids possess permanent dipole movement, they absorb infrared radiation of sunlight. Due to the same dipole movement property, water (a greenhouse effect causing liquid) present in a plant leaf gets evaporated due to the absorption of infrared radiation part of sunlight falling on the plant leaves surfaces into the atmosphere through the fine pores present in those plant leaves [1,131]. This process is popularly known as *transpiration*, which is similar to the *respiration* process performed by human beings. The occurrence of this *transpiration* process is a must to release of the molecular oxygen (O_2) formed in the water oxidation reaction (photosystem-II) of *natural photosynthesis* (NP) process into the atmosphere through the pores present in the plant leaves. This *transpiration* process also facilitates the breathing of CO_2 gas from the atmosphere by plant leaves to perform the *photosystem-I* reactions of *NP* process to store solar energy in the form of bio-mass and food materials. Nevertheless, the efficiency of *NP* will never exceed 1% given the concentration of CO_2 in the atmosphere is around only 400 ppm today [1].

2. Experimental section

2.1. Fabrication of a SLAPE solar panel

A SLAPE solar panel 100 fabricated by using 21 numbers of SPVCs as semiconducting material, γ-butyrolactone as a non-working fluid to absorb the sunlight and to generate heat-energy out of the absorbed sunlight in conjunction with SPVCs, and dichloromethane (DCM) as a working fluid is shown in Fig. 7 (a & b) along with a block-diagram Fig. 7 (c) showing three major parts utilized by SLAPE solar panels in generating electricity from sunlight [1,126]. The SLAPE solar panel captures >90% of the sunlight reaching the earth surface and converts it into heat-energy, which can be eventually turned into electricity by using organic Rankine cycle (ORC) with the help of an heat-engine and electric generator. The possible beneficial properties of SLAPE solar panels in comparison to those of SPVC solar panels are given in Table 4. The further details of this SLAPE solar panels construction is well illustrated in the schematic drawings shown in Figs. S1-S6 [1,126], in which, some reference numerals are given to indicate each and every part used in the fabrication of SLAPE solar panel shown in Fig. 7 (a & b). In Figs. S1 & S2, the parts 101 and 112 are two-numbers of the stainless steel (SS-304) frames with rectangular shape having outer-outer dimensions of ~1520 mm length × ~700 mm width welded out of ~33 mm width × ~5 mm thick flat plate bars by using the tungsten inert gas (TIG) welding technique [1]. Each of these two frames were made to have three equally spaced openings for light transmission using two numbers of either flat plate tee (T) shaped (Fig. 7(a)) or just flat SS-304 bars 113 (Fig. 8) having dimensions of ~634 mm length × 33 mm width × 5 mm thick that divide that single major rectangular shape frame into three small size rectangular shaped openings. The T-shaped bars 113 at the centre portion of the SLAPE solar panel 100 can be seen from its digital photo (Fig. 7). Each of the SS frame was made with 36 numbers of 12 mm diameter (ϕ) holes 125 (Figs. S3 & S4) [1,126], which are used to hold all the parts of the SLAPE solar panel 100 together while forming two numbers of gas-tight top and bottom chambers with the help of M10 size studs 116 and

Preprints (www.preprints.org) | NOT PEER-REVIEWED | Posted: 15 November 2023 doi:10.20944/preprints202311.0965.v1

117 (Fig. S2) tightened using two-numbers of nuts 120 on both top and bottom sides after placing both rubber 118 as well as metal 119 washers between the frame and the nuts fitted to the studs.

Table 4. Major possible advantages of SLAPE solar panels when compared with the commercial silicon photovoltaic cell (SPVC) solar panels [1].

S. No.	Advantage
1.	It exhibits all the benefits that are exhibited by SPVC.
2.	In comparison to SPVC, it is economical and stable as it need not have to employ the expensive materials like crystalline Si solar cells.
3.	Unlike SPVC, it does not consider only 70% sunlight for electricity generation.
4.	Unlike SPVC, its voltage generation is not limited to only 0.7 V.
5.	Unlike SPVC, its conversion does not decrease with increasing ambient temperature.
6.	Unlike SPVC, it does not block 8 to 10% light conversion into electricity by electrically conducting metal linings on cells.
7.	Unlike SPVC, it need not have to be irradiated with straight light.
8.	Unlike SPVC, it does not use toxic heavy metals like Pb.
9.	Unlike SPVC, there would not be any after use disposal problem.
10.	Unlike SPVC, it does not create any local heat island effect.
11.	Unlike SPVC, it is reusable and physically robust.
12.	Unlike SPVC, its efficiency does not decrease by 1% each passing year.
13.	Unlike SPVC, it does not reflect 40% sunlight falling on its surface when black Si wafers are employed in them.
14.	Unlike SPVC, it needs regular maintenance like locomotive steam engines need.

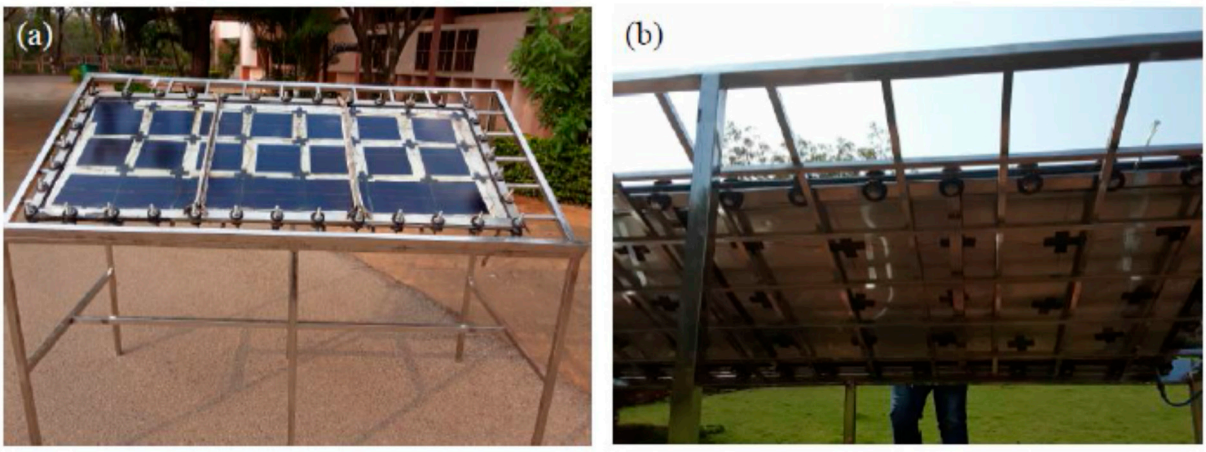

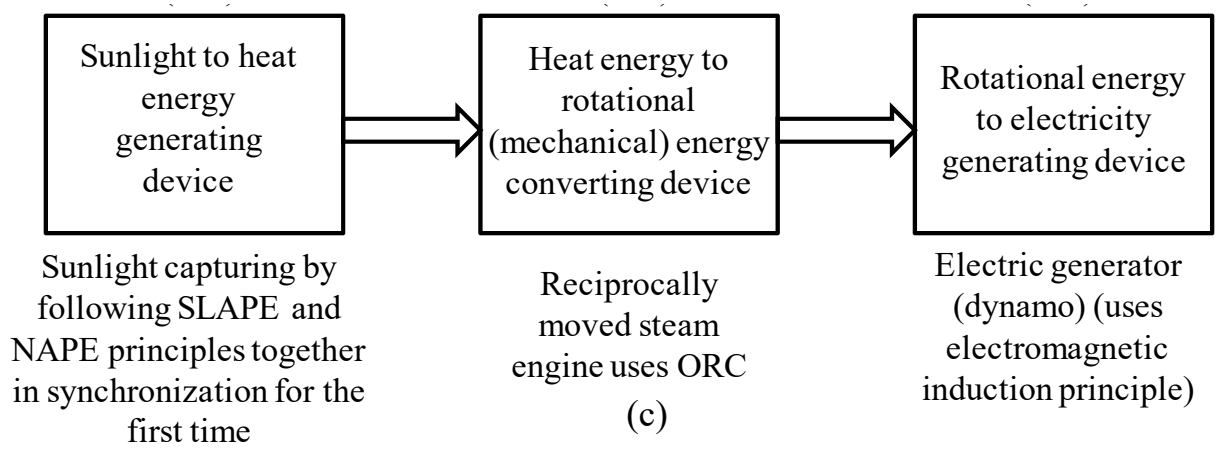

(c)

 doi:10.20944/preprints202311.0965.v1

Figure 7. A digital photograph of the sunlight-to-heat energy generating SLAPE solar panel. Panel is placed with an inclination of 30°; (a) front view, and (b) rear view; (c) block diagram showing the generation of electricity from sunlight using a SLAPE solar panel [1,126].

Figure 8. The volume of the SLAPE solar panel **100** before (a) and after (b) exposing to the sunlight for more than 60 minutes when the 0.5 mm thick Al sheet was employed to separate the top and bottom chambers, where the top chamber containing 21 SPVCs immersed in 9.6 litres of γ-butyrolactone (NWF **123**). The average solar insolation was about 80 mW/cm^2 and the average room temperature was about 28°C [1].

The SLAPE solar panel 100 had with two-numbers of gas tight chambers created by using 3 numbers of *Viton* 102, 105, and 111, and one *ethylene propylene diene monomer (EPDM)* 109 gaskets with dimensions of 15 mm width × 1.5 mm thick Fig. S2 [1,126]. The top chamber is formed between the low-iron containing fully transparent, fully toughened and one-side surface-grooved Borosil solar glass (1480 mm length × 660 mm width × 3.2 mm thick) sheet 110 (supplied by *M/s. Gujarat Borosil Ltd., India*) placed on top side, and a thin and highly thermally conducting 0.5 mm thick Al, 1.1 mm thick or 0.2 mm thick Cu sheet (1480 mm length × 660 mm width) 106 placed on bottom side. Since, the Cu sheet with 0.2 mm is available with only 350 mm width in Hyderabad, India, two sheets of 350 mm width were silver brazed together by keeping them side-by-side to form a 660 mm width and 1480 mm length sheet. The four sides of this gas-tight top chamber is closed with EPDM rubber gasket 109, and to maintain the gap in between top side solar glass sheet 110 and bottom side thermal conducting thin metal sheet 106, 21 numbers of EPDM rubber pieces 108 (~60 mm × 60 mm size cut into plus (✚) shape with 20 mm projections) were utilized. The T-shaped flat plate bars used in the construction of SLAPE solar panel (Fig. 7) does not allow the swelling of the centre portions of the top-chamber when the volume of the low-boiling point DCM working fluid present in the bottom chamber expands by absorbing the *in situ* generated heat energy by the SPVCs and γ-butyrolactone [1,126]. In the top chamber, Viton gasket or gap-maintaining pieces cannot be placed as it gets swelled when it comes into contact with γ-butyrolactone NWF 123 solvent employed in the top chamber along with semiconducting materials to capture the sunlight. However, EPDM is quite compatible with the γ-butyrolactone NWF 123 solvent. The 21 numbers of EPDM pieces were joined together using 0.5 mm thick diameter (ϕ) Cu wire 115 (Fig. S3) and the extended portions of this Cu wires 115 were

secured by placing them in between the two SS frames (101 and 112) tightened with nuts and studs [1,126]. The volumes of these chambers can be varied from 2 litre to 10 litres with the help of two numbers of joints that give three equally spaced opening to the frames 101 and 112.

In this top chamber, 21 numbers of multi-crystalline silicon (Si) photovoltaic cells (SPVCs) 107 (15.7 cm × 15.7 cm × <0.25 mm) (Grade A type – P157 × P157, power 18.0%) (supplied by M/s. Adani Solar India, Ahmedabad) interconnected with Sn-Pb (Sn60/Pb40) coated Cu (~1.3 mm width × 0.2 mm thick) (supplied by M/s. the PV connect, IDA Nacharam, Hyderabad) strip 121 (Fig. S4) were also secured tightly by placing the interconnecting Cu stripes mechanically held in between the SS frames 101 and 112. This top chamber containing SPVCs was filled with either 2.3 litres or 9.6 litres of γ-butyrolactone NWF 123 using 12 mm diameter holes (ϕ) provided on top side solar glass at diagonals, and fitted with SS-304 pipes and needle valves 114 (Figs. S2, S3 & S4) [1,126]. 100 mL volume glass syringe with SS needle was used to fill this top chamber with γ-butyrolactone NWF 123 solvent. As soon as, the top chamber is filled with γ-butyrolactone (NWF 123) solvent, the glass syringe with needle was removed, and the tightened tie-rod studs and nuts fully seal the gap so as to not to leak γ-butyrolactone (NWF 123) solvent from top chamber.

The gas-tight bottom chamber was formed between the top-side thin metal sheet 106 and bottom-side fully toughened soda lime glass sheet 103 (1480 mm length × 660 mm width × 5 mm thick; supplied by *M/s. Safe Glass Store, Hyderabad, India*), which was also provided with two-numbers of 12 mm diameter (ϕ) holes at two-diagonal ends to fix an SS-304 cylindrical shaped pipes 104 with dimensions of 10 cm length × 12 mm outer diameter × 10 mm inner diameter, and one end of the pipe was given with an inner threading to fit a needle valve so as to use it as an inlet and outlet for working fluid (WF) 124 dichloromethane (DCM). To form the gas tight chamber, the Viton rubber gasket 105 was used, and to maintain the gap in this chamber, 21 numbers of Viton rubber pieces 122 (21 numbers of ~60 mm × 60 mm size cut into plus (✚) shape with 20 mm projections) (Fig. S4) were utilized. This bottom chamber is filled with dichloromethane (DCM) WF 124 using inlets and outlets 104 (Fig. S2) [1,126]. The Viton rubber is quite compatible with dichloromethane (DCM) WF 124 solvent.

In order to adiabatically seal this the SLAPE solar panel 100 from its surroundings, the top surface of the low-iron containing 3.2 mm thick Borosil solar glass was covered with a 0.13 mm adhesive coated fluorinated ethylene propylene (FEP) film (3D Techno, Gujarat, India; A4 size sheet & without adhesive FEM film with the dimensions of 0.15 mm × 300 mm × 3000 mm), followed by three layers of 0.15 mm thick fully transparent polyethylene terephthalate transparent (PET) plastic sheet, and then by another 0.32 mm Borosil low-iron containing solar glass to arrest the heat loss from the top glass, and the bottom 5 mm thick sodalime glass 103 surface of the bottom chamber of the SLAPE solar panel 100 was covered by two numbers of 3 mm thick silicone rubber sheet 128 followed by 0.5 mm stainless steel (SS) metal sheet 129 in order to minimize the heat losses that occur to the surroundings *via* convection, convention, and radiation processes due to the presence of temperature gradient between the SLAPE solar panel 100 and its surroundings [1,126]. The reduction in the intensity of the sunlight from diathermanous material covering given on Borosil solar glass surface has been measured to be less than 15%. These diathermanous covering materials including silicone rubber 128 and metal 129 sheets are not shown in any of the figures for the purpose of clear view of the inner parts of the SLAPE solar panel 100. The pipes and tubes, which make up the conduit in the SLAPE solar panel 100, and the fluid passageways between the various components of the heat generating system are connected and integrated using compression fittings so as to prevent the leaks of both NWF 123 and WF 124. The global normal transmission coefficient of 3.2 mm thick Borosil solar glass sheet 110 is about 0.91. Usually, for double-side anti-reflection coated low-iron solar cover glass, the transmission coefficient is higher than 0.94. The standard test conditions for measuring the efficiency of the SLAPE solar panel 100 are the temperature of 25°C, and an irradiance of light with a power density of 1000 W/m² (1 kW/m² or 100 mW/cm² or air-mass 1.5 (AM1.5) [1,126].

2.2. Fabrication of reciprocally moved steam engine

Preprints (www.preprints.org) | NOT PEER-REVIEWED | Posted: 15 November 2023 doi:10.20944/preprints202311.0965.v1

The details, a digital photo revealing partial details and schematic diagram of reciprocally moved steam engine (RMSE) **200** employed in this investigation to convert the *in situ* generated heat energy into rotational mechanical energy is shown in Fig. S5 [1,126]. The WF **124** with a minimum pressure of >1.5 bar leaves the bottom chamber of the SLAPE solar panel **100** *via* a controlled valve into the steam chest **201** of RMSE **200** thereby it moves into the main cylinder **202** *via* inlet or outlet ports **207**, and causes the movement of the piston **203** in the main cylinder so as to move it reciprocally with the help of the eccentric plate **221** connected to the main cylinder piston *via* a connecting rod **218** (or joint) and axle **219**. When the eccentric plate **221** connected to the crank shaft **220** causes the rotation of another eccentric plate **223** sat on the crank shaft **220** adjacent to the eccentric plate **221** that is connected to the main cylinder piston [1,126]. When this latter eccentric plate **223** rotates, it also moves the sliding D valve cum piston rod (**210** & **211**) in the steam chest cum sliding D-valve chamber with the help of the connecting rod **213**. The pitons (**203** & **211**) and the **218** & **213** connecting rods are joined with the help of two numbers of cross head bearings **204** and **212**, respectively. When both the pistons **203** and **211** are reciprocally moved, they cause the entering and exit of the WF **124** vapor *via* ports **207** and **208**, respectively. The one-side dead-end of the piston **203** causes the pushing off of the WF **124** vapor out of the main cylinder *via* exhaust port(s) **207**, when it gets aligned with the opening ports of the centre hole **208** given to the piston connected to the steam chest cum sliding D-valve chamber **209**. The main cylinder is connected to the steam chest cum sliding D-valve chamber **209** as shown in Fig. S5 using silver brazing technique and this latter assembly is fixed to a stand **215**, which in turn is fixed to a base plate **217** using screws **214** and **216**. The crank shaft **220** and flywheel **225** are fixed to the base plate **217** using two-numbers of holders **222** with the help of screws **224** [1,126].

2.3. Fabrication of electric generator

A custom made electric generator **300**, whose schematic diagram given in Fig. S6 was attached to the crankshaft **220** of the reciprocally moved steam engine **200** (Fig. S5) to generate electricity according to the principles of *Faraday and Lenz laws of electromagnetic induction* when the WF **124** vapor causes the movement of pistons (**203** & **211**) by entering *via* the steam chest port **201** of RMSE **200** [1,126]. The electric generator used in this study to generate electricity from sunlight consists of 4 numbers of rare earth neodymium (NdFeB) ($Nd_2Fe_{14}B$) super strong magnets (50 mm length × 10 mm width × 7 mm thick) **301**, which are firmly fixed in the four slots made on a machined nylon rod **302** (40 mm diameter (ϕ) and 50 mm length) as schematically shown in Fig. S6 [1,126]. At the centre of this nylon rod **302**, a hole of 5 mm diameter is made so that it can firmly sit on the crankshaft rod **220** of the RMSE **200**. The nylon rod **302** fixed with four numbers of super strong magnets **301** was placed at centre and equidistance from either four or two Cu coils **303**, which are fixed to 6 mm thick transparent polypropylene (PP) sheets **304** so that the magnets **301** placed on nylon rod **302** are easily rotated with the crankshaft **220** of the RMSE **200** at centre of these four or two Cu coils. The Cu coils are made by winding 1500 cycles of 0.2 mm diameter (ϕ) insulated wire on a PP piece of 3 mm thick × 8 mm width × 50 mm length (these PP pieces are not shown in any of the schematic diagrams for clarity purposes) [1,126]. These four or two numbers of 1500 turns containing Cu coils are firmly fixed to the 3 mm thick plastic sheet **305** that is fixed to the base using super strong glue (quick fix solution) with the help of 6 mm thick transparent PP legs **306** [1,126].

3. Results and discussion

3.1. Effects of parameters variation on the performance SLAPE solar panels

The SLAPE solar panel **100** as shown in Fig. 7 (a & b) was exposed to the sunlight by placing it on an metal stand **126** at an inclination of 30° while facing the south side between 11 am and 3 pm during the sunny days of the first-half of March month of 2020, where the average powder density of the irradiated sunlight and the average room temperature of the surrounding atmosphere were measured to be ~80 mW/cm^2 and ~28°C, respectively [1,126]. The dimensions of the SLAPE panels chosen for this study was based on the solar glass sheets available in the market and to have at light

capturing area of least one square meter as it receives about one kWh equivalent sunlight in an hour time. This is the minimum area required to generate required pressure in DCP WF to rotate the armature of the electric generator fixed on crank shaft of RMSE to produce the measurable electricity by using a multimeter. The amount of *γ-butyrolactone* and the number of SPVCs present in the top-chamber of SLAPE solar panel shown in Fig. 7 are ~ 9 litres and 21, respectively, whereas, the bottom chamber had 2 litres of DCM WF. The heat-energy *in situ* generated by *SPVCs* and *γ-butyrolactone* upon exposure to sunlight has passed from top-chamber to bottom chamber through the 0.5 mm thick Al metal sheet. A video (video S1) showing the boiling of DCM solution upon receiving the *in situ* generated heat energy by SPVCs and *γ-butyrolactone* together and passing of thus generated heat energy from top-chamber to bottom chamber through 0.5 mm thick Al sheet that has separated these two chambers of SLAPE solar panel (Fig. 7) is given in the supporting information). The results obtained under various experimental conditions employed are given in Table 5. The 0.2 mm thick copper sheet possesses four time higher thermal conductivity when compared with the 0.5 mm thick Al sheet as the thermal conductivity of the Al is half-of-the one exhibited by Cu metal. The beneficial effects of using 0.2 mm thick Cu sheet in this SLAPE solar panel can be seen from the results summarized in Table 5.

However, when the solar panel shown in Fig. 7 was exposed to sunlight, it started to get swelling considerably as shown in Fig. 8 (a) & (b), and within two hours of its exposure, it got swelled in such a way that it might explode if this exposure is continued for some more time [1]. To avoid the explosion, the top-solar glass surface of the SLAPE solar panel (Fig. 7) was immediately covered with a black rubber sheet completely to avoid the falling of sunlight on its top surface. Furthermore, to avoid swelling of the chambers of the SLAPE solar panel, the flat shaped SS 304 frames (Fig. 8 (a) & (b)) used as tie-rods were replaced with T-shaped ones as can be seen from Fig. 7 (a), and to avoid heat-loss through the bottom transparent soda-lime glass sheet as can be seen from Fig. 7 (b) and its breakage, it was supported with two-layers of 3 mm thick EPDM rubber sheet followed by 0.5 mm thick SS sheet, and in place of 0.2 mm thick Cu sheet, a 1.1 mm thick Cu sheet was employed. When this modified SLAPE solar panel was exposed to sunlight, within 2 hours' time, the top light transmitting solar glass got exploded completely, and all the solutions from both top and bottom chambers have come out of the SLAPE solar panel as considerable amount of pressure generation was noted inside the panel as the swelling of both top and bottom chambers and the loss of heat transfer from bottom side were almost restricted. The high pressure *in situ* generated has severely bent the 5 mm thick SS-304 frames and 1.1 mm thick Cu sheet as can be seen from Fig. S7 (a-d). This incident can be considered as a proof of the absorbance of sunlight by the *SPVCS* cells when fully immersed in *γ-butyrolactone* and generating heat-energy out of the absorbed sunlight to boil and increase the volume of DCM working fluid present in the bottom chamber. In this case, all the generated pressure can be attributed only to the evaporation of DCM WF as *γ-butyrolactone* (non-working fluid, NWF), does not generate any pressure below 50°C as its boiling point is 200°C [1].

After the SLAPE panel got exploded, a Cu tube conduit (Fig. S8) fabricated out of 3/8th diameter Cu tube was used to store the *DCM* WF instead of directly in the rectangular shaped bottom chamber formed between Cu and glass sheets. It was found that the rectangular shaped chambers cannot withstand high pressures without undergoing any deformation (in this case swelling), and only cylindrical shaped tubes can withstand such pressures without undergoing such dimensional changes. Probably that could be the reason behind using cylindrical shapes for all the pressure tanks and cylinders. In fact, the cylinder shape does not allow any deformation but rather it gets exploded when the inside pressure exceeds the withstanding limits of the construction material. Since, the Cu sheet employed had a thickness of 1.1 mm, the Cu conduit tube could be easily brazed to it without allowing the formation of any pin-holes and to increase the required heat transfer from top-chamber to the bottom-chamber (i.e., from *γ-butyrolactone* non-working fluid (NWF) to the dichloromethane (DCM) working fluid (WF)) [1].

The modified SLAPE solar panel shown in Fig. 9 (a & b) exhibited (video S2) a voltage generation of about 16 V electricity with alternating current (AC) when exposed to sunlight for about two-hour time with the help of a RMSE (Fig. S5), and a custom-made four magnets containing electric generator

Preprints (www.preprints.org) | NOT PEER-REVIEWED | Posted: 15 November 2023 doi:10.20944/preprints202311.0965.v1

(Fig. S6). The generation of 16 V electricity by this modified SLAPE solar panel can be seen in the video (video S2) given in the supporting information. The 21 SPV cells present in this SLAPE solar panel actually generates only 10 V DC electricity when they are connected in series in a commercial SPVC solar panel. However, the same 21 SPV cells in this SLAPE panel generated 16 V electricity with AC current even when the electric generator was not fabricated according to the standard design procedure. Furthermore, in another experiment conducted on 28th and 29th days of March 2022 using this modified SLAPE solar panel with 30 SPV cells, the generation of pressure exceeding the reading capabilities of the pressure gauges (>30 bar) can also be seen from Fig. S9 (a & b). The glowing of a 5 W LED bulb with the pressure generated by this modified SLAPE solar panel containing 30 SPV cells with the help of a commercially available small-size DC generator can also be seen from Figs. S10 & S11. The amount of current generated is not measured, because these experiments were aimed only to show the *proof of concept (PoC)* of SLAPE and as there is huge heat-loss associated with the present SLAPE solar panels, which does not allow the true electricity generating capability of SLAPE solar panels.

Figure 9. (a) SLAPE solar panel containing about 30 SPV cells with a packing factor of about 100% and about 2 litres *γ-butyrolactone* solution and (b) the SLAPE panel connected with reciprocally moved steam engine (RMSE) but not with electric generator [1].

In order to establish that the SPVCs and *γ-butyrolactone* are needed together to turn sunlight into heat-energy, the control experiments were also conducted. For this purpose, three SLAPE solar panels with same dimensions and using similar components were fabricated. One SLAPE solar panel had both 30 SPV cells and 2 litres *γ-butyrolactone* in the top-chamber, the second SLAPE panel had only 30 SPV cells in the top-chamber, and the third SLAPE panel had neither SPV cells nor *γ-butyrolactone* in the top-chamber. These three SLAPE solar panels had about 1.8 litres DCM solution in the bottom chambers of their copper conduits. These three SLAPE solar panels were exposed to sunlight on 5th January 2022. The pressures generated in the gauges attached to the manifolds of copper conduits are plotted and given in Fig. 10. It can be seen that to generate the required pressures to rotate the reciprocally moved steam engine piston to generate electricity both SPV cells and *γ-butyrolactone* are compulsorily required, and neither only SPV cells nor the empty top-chamber generate pressures higher than 1 bar. On 25th February 2022 (i.e., on a normal sunny day), when a SLAPE solar panel (Fig. S11 (a-g)) was exposed to the sunlight and measured the temperature of its top glass surface by placing the tip of the thermometer on its top surface, a reading of about 47°C was noted (video S3 in supporting information), which is about 14°C higher temperature than that of ambient room temperature of that day at about 13:30 hours (about 34°C). Surprisingly, during the measurement, a small wind-blowing was also noticed for few seconds, immediately, a reduction of about 2°C temperature in the thermometer reading was noted. It clearly indicates that there is a continuous loss of in situ generated heat into the atmosphere by means of conduction, convection and radiation through the top glass surface due to the temperature difference between SLAPE solar panel glass

Preprints (www.preprints.org) | NOT PEER-REVIEWED | Posted: 15 November 2023 doi:10.20944/preprints202311.0965.v1

surface and its surroundings. This heat loss is the top-most obstacle at present preventing the achievement of higher sunlight-to-electricity (STE) generating conversion efficiency. The second major obstacle is the steam engine employed in these experiments is a laboratory model device designed for engineering students' experiments purpose, which is associated with huge pressure losses from the piston-cylinder openings. At present the atmospheric weather conditions such as, ambient temperature, wind speed and its direction, humidity in the atmosphere, etc., were found to have a profound effect on the output of these SLAPE solar panels. However, their efficiency is supposed to be affected by only solar radiation but not with the atmospheric conditions. To avoid these effects, a completely adiabatically sealed SLAPE solar panel is being fabricated. Further to avoid, the sunlight reflection losses, the SPVCs will be replaced with thin black silicon wafers as these wafers do not reflect any visible light falling on them. In fact, these black silicon wafers absorb the complete sunlight reaching the earth surface with wavelength ranging from 250 nm to 2400 nm with their using surface texture. It is called black silicon because it does not reflect any light falling on it as a blackbody radiation [1].

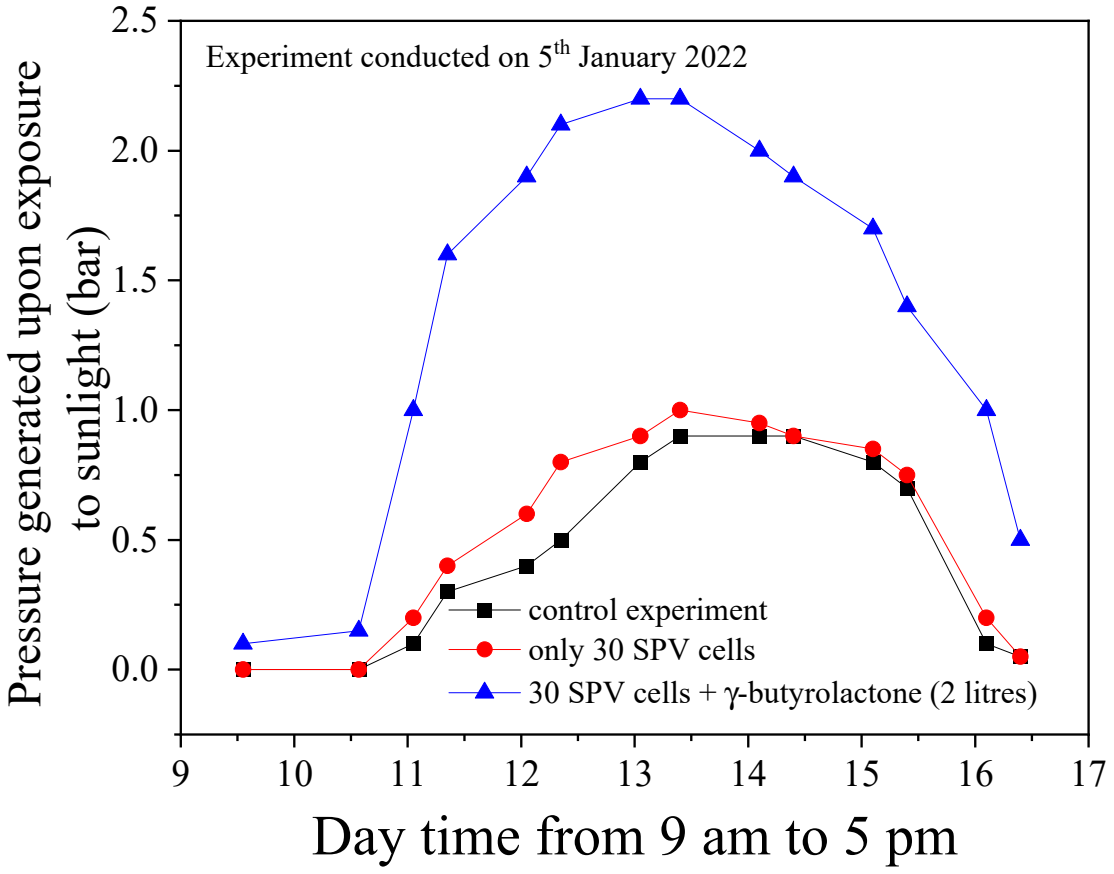

Figure 10. Pressures noted in the gauges attached to the copper conduits of SLAPE solar panels when their top-chambers had different sunlight absorbing contents. Experiment was conducted on 5th January 2022 at ARCI, Hyderabad campus [1].

The considerably high thermal conductivity of Borosil solar glass could be responsible for the higher amounts of *in situ* generated heat loss occurring through the SLAPE solar panel to the atmosphere. In fact, high thermal conducting solar glass is required for SPVC solar panels but not for SLAPE solar panels. For *SPVC* solar panels this highly thermal conducting Borosil solar glass is compulsory for dissipating the *in situ* generated heat by *SPV* cells as soon as possible as their efficiency is inversely proportional to the operating ambient temperature. This is the reason for the local heat island effect normally seen wherever large number of *SPVC* solar panels are deployed. However, the SLAPE solar panels need glass sheets with lowest possible thermal conductivity. In the control (i.e., blank) experiment, where, the SLAPE panel did not had any *SPVCs* or *γ-butyrolactone*,

Preprints (www.preprints.org) | NOT PEER-REVIEWED | Posted: 15 November 2023 doi:10.20944/preprints202311.0965.v1

the temperature measured on the top Borosil solar glass surface was no different from the one measured at ambient room temperature although certain pressure was noted the Cu conduit containing DCM WF. These results clearly suggest that the semiconducting materials along with a suitable solvent are compulsory to capture the sunlight and to turn it into the heat-energy. When wind was blowing, the increased heat-loss was also noted. In fact, the entire SLAPE technology is based on the heat-energy *in situ* generated from sunlight before converting it into electricity. Now in these present SLAPE solar panels, most of the *in situ* generated heat energy is continuously losing into the atmosphere. Unless such leakages are completely arrested, it is not possible to achieve the desired conversion of STE efficiency for these SLAPE solar panels.

3.2. The theoretical efficiency vs. experimentally generated results

The specific heat capacity (Cp) and materials weights involved in the experiment conducted as per the 2nd row of Table 5 are given in Table 6. When the top and bottom-chambers of the SLAPE solar panel **100** (Fig. 7) were filled with about 2.3 litres of γ-butyrolactone (NWF **123**) and about 2 litres of DCM (WF **124**), respectively, and then exposed to the sunlight from 11 am to 3 pm (i.e., for 4 hours duration) continuously on the 13th March 2020 at ARCI, Hyderabad, Telangana, India, on that day the recorded room temperature at about 11 am and the average power density of the irradiated sunlight were measured to be ~ 28°C and ~80 mW/cm², respectively. The amount of total sunlight that fell on the surface of the SLAPE solar panel **100** during 4 hours period can be calculated as follows:

$\Rightarrow$ 80 mW/cm² = 800 W/m² = 0.8 kW/m² = 0.8 kWh/m² (for 1 hour duration); $\Rightarrow$ 0.8 kWh/m² × 4 hours = 3.2 kWh.

Table 5. The various reaction conditions and the values of sunlight-into-heat energy generated by SLAPE solar panels.†.

Light capturing system	Non-working fluid (NWF) **123** (litres)	Metal that separates the top chamber from bottom chamber	Heat insulation given on top and bottom glasses (yes or no)	Temp. (°C) & pressure (bar) noted in WF **124** after 120 minutes of exposure to sunlight (± 2.0)⊥
Si solar cells + γ-BL	2.3	Al (0.5 mm	No	~54 & 0
Si solar cells + γ-BL	10	Al (0.5 mm)	Yes	>40 & ~1.0
Si solar cells + γ-BL	2.3	Al (0.5 mm)	Yes	>40 & >1.0
Si solar cells + γ-BL	2.3	Cu (0.2 mm)	Yes	>40 & >1.5
Si solar cells	0	Cu (0.2 mm)	Yes	>40 & <1.5
Si solar cells + γ-BL	10	Cu (0.2 mm)	Yes	>40 & >3.0

† γ-BL stands for γ-butyrolactone; DCM stands for dichloromethane; ‡In these experimental conditions, within two-hours of exposure to the sunlight, a lot of swelling of the device at centre portion of the SLAPE panel **100** was noted.; if it was further exposed to the sunlight without opening the valve connected to the bottom chamber containing the DCM WF **124**, the device would have been exploded since that kind of pressure generation and swelling of the device was noted.; ⊥The temperature and pressure values were measured using a thermometer and pressure gauge, respectively.

Table 6. The specific heat capacity and weights of various materials employed in the fabrication of SLAPE solar panels.

Material	Specific heat capacity (kJ/kg·°C)	Weight (grams)	Density (g/cm³)
Silicon solar cells **107**	0.71	~11.9×21 = 249.9	2.33
Copper sheet (0.2 mm thick) **106**	0.385	~1750	8.96
Aluminum sheet (0.5 mm thick) **106**	0.90	~1020	2.70
γ-Butyrolactone (NWF **123)**	1.642	~2576 (2.3 litres)	1.12
Dichloromethane (DCM) (WF **124)**	1.188	~2660 (2 litres)	1.33

 doi:10.20944/preprints202311.0965.v1

Water	4.20	-	1.00

The total sunlight capturing active area of the SLAPE solar panel **100** employed was:
⇒ (1464 mm × 644 mm; total panel rectangular area) – (33 mm × 644 mm × 2 numbers; it is the area covered by tee (T)-shaped bars **113** used to divide the rectangular SS frames into three equally spaced openings)
⇒ 9428.16 cm^2 – 425.04 cm^2; ⇒ 9003.12 cm^2;
⇒ 0.9003 m^2

The total area of sunlight that can be captured by 21 numbers of multicrystalline silicon (*mc-Si*) cells **107** in SLAPE solar panel **100** was:
⇒ (15.7 cm × 15.7 cm × 21 numbers) – (33 mm × 644 mm × 2 numbers; it is the area of T-shaped bars **113**) – (8% area covered by grid and bus-bar lines printed on the surface of SPV cells)
⇒ 5176.29 cm^2 – [400 cm^2 + 414.10 cm^2]
⇒ 5176.29 cm^2 – 814.10 cm^2
⇒ 4362.19 cm^2
⇒ 0.4362 m^2

The packing factor is termed as the total sunlight capturing *mc-Si* cells **107** area divided by the total active sunlight capturing SLAPE solar panel **100** area is as follows:
⇒ 0.4362 m^2 / 0.9003 m^2
⇒ 0.4845

The total amount of sunlight that could be captured by the SLAPE solar panel **100** can be determined as follows: As the 10% of the sunlight falling on the panel is normally reflected by the top Borosil solar glass **110**, and if another 10% miscellaneous losses are considered, then the remaining 80% light can be captured by the SLAPE solar panel **100**. The 80% of 3.2 kWh is equal to 2.56 kWh (= 3.2 kWh × 0.8). Out of which, the amount of light energy to be captured at a rate of 30% by γ-butyrolactone (NWF **123**) solvent present in the area of 0.9003 m^2 is equal to 0.691 kWh per 0.9003 m^2 area in 4 hours experiment duration (= 2.56 kWh × 0.9003 m^2 × 0.3). The amount of light that is captured by silicon solar cells at a rate of 70% is equal to 0.7816 kWh (= 2.56 kWh × 0.4362 m^2 × 0.7). The total solar energy that could be captured by the SLAPE solar panel **100** is equal to 1.4726 kWh (= 0.7816 kWh + 0.691 kWh).

The captured sunlight energy (i.e., 1.4726 kWh) amounts to only about 57.52% of the solar energy (i.e., 2.56 kWh) fell on the 0.9003 m^2 surface area of SLAPE solar panel **100** during 4 hours period. If nano-size amorphous silicon powder was placed in place of *mc-Si* cells in 0.9003 m^2 area with γ-butyrolactone (NWF **123**) solvent so as to appear like a liquid crystal display (LCD) screen, instead of 57.52%, it would have been 100%.

On the other hand, the amount of energy required to raise the temperature of the contents of the SLAPE solar panel **100** by 1°C can be derived using Eq. 2.

$$Q = Cp * m * dT \qquad (2)$$

Where, the Q is the amount of energy (in kJ) required to raise the temperature (dT) of the contents having a mass of m kgs. As per the data given in Table 6, the heat capacity of the entire four major heat capturing materials (i.e., multicrystalline silicon (mc-Si) solar cells **107**, γ-butyrolactone (NWF) **123**, Al sheet **106**, and dichloromethane (DCM)) (WF) **124** present in the SLAPE solar panel **100** as per reaction conditions given in 2nd row of Table 5 can be derived as follows:
⇒ 0.71 kJ/kg*°C × 0.2499 kg × 1 °C for pc-Si + 0.90 kJ/kg*°C × 1.02 kg × 1 °C for Al metal sheet + 1.642 kJ/kg*°C × 2.576 kg × 1 °C for γ-butyrolactone + 1.188 kJ/kg*°C × 2.660 kg × 1 °C for DCM
⇒ 0.177429 kJ + 0.918 kJ + 4.2299 kJ + 3.16008 kJ
⇒ 8.4854 kJ.

The amount of heat energy (kJ) required to raise the temperature of the heat capturing materials involved in experiment conducted as per the reaction conditions given in 2nd row of Table 5 by 1 °C is about 8.4854 kJ. The amount of solar energy that can be captured by both c-Si **107** + γ-butyrolactone (NWF **123**) is about 1.4726 kWh, which is equivalent to 5297.122 kJ since 1 kJ = 0.000278 kWh. Whereas, to raise the temperature by 1°C of the heat capturing materials of the SLAPE solar panel

Preprints (www.preprints.org) | NOT PEER-REVIEWED | Posted: 15 November 2023 doi:10.20944/preprints202311.0965.v1

100 needs the energy of about 8.4854 kJ. In that case, 5297.122 kJ (i.e., the total solar energy captured by the SLAPE solar panel **100**) can raise the temperature of the contents by 624.26°C (= 5458.63 kJ/8.4854 kJ) if there is no loss of heat energy to the surroundings. That means at the end of reaction conducted for about 4 hours under the irradiation of sunlight at a power density of 80 mW/cm^2, when there was no loss of the *in situ* generated heat, then the total temperature of the contents of the SLAPE solar panel **100** should reach a temperature of 624.26°C at a rate of heating of 2.60°C per minute (=624.26°C/240 minutes). Since, the initial temperature (i.e., room temperature) of the heat absorbing materials on the 13th day of March 2020 at ARCI, Hyderabad, Telangana, India, was about 28°C during the starting of the experiment at 11 am, to reach the boiling temperature of DCM (WF **124**) (i.e., 40°C), about 4.6158 minutes is required (i.e., 40°C–28°C = 12°C; when the temperature of the contents is raised at the rate of 2.935°C per minute (4.477 minutes = 12°C/2.60°C per minute) if the heat transfer from γ-butyrolactone (NWF **123** present in the top-chamber) through 0.5 mm thick Al metal sheet **106** to DCM (WF **124** present in the bottom chamber) is immediate. However, it took about 14 minutes time to start boiling of the DCM (WF **124**) in the bottom chamber after exposing the SLAPE solar panel **100** to the sunlight.

The amount of vapor pressure that can be generated out of DCM (WF **124**) upon exposure to 100°C during the experiment can be derived theoretically by using the Clausius-Clapeyron equation is given in Eq. 3.

$$\ln\left(\frac{P_1}{P_2}\right) = -\frac{\Delta H_{vap}}{R}\left(\left(\frac{1}{T_1}\right) - \left(\frac{1}{T_2}\right)\right) \qquad (3)$$

Where, P_1 (134 mmHg or 134 torr) is the vapor pressure of DCM (WF **124**) at temperature at 0°C or 273.15 K (T_1); P_2 is the vapor pressure of the DCM at temperature at 100°C or 373.15 K (T_2); ΔH_{vap} is the enthalpy of vaporization of DCM, which is equal to about 2850 J.mol^{-1}); and R is the universal gas constant, about 8.314 J. mol^{-1}. K^{-1}. As the temperature gradient between the NWF **123** (γ-butyrolactone) and WF **124** (DCM) increases, the heat transfer from NWF **123** to WF **124** takes place *via* 0.2 mm thick Cu sheet **106**.

The value of P_2 can be determined as follows:

$$\Rightarrow \ln\left(\frac{P_1}{P_2}\right) = -\frac{30855.104}{8.314}\,(\text{J.mol}^{-1}/\text{J.mol}^{-1}.\text{k}^{-1})\left(\left(\frac{1}{273.15}\right) - \left(\frac{1}{373.15}\right)\right)\,(\text{k}^{-1})$$

$$\Rightarrow \ln\left(\frac{P_1}{P_2}\right) = -\,3711.210\,(\text{J.mol}^{-1}/\text{J.mol}^{-1}.\text{k}^{-1}) \times 0.00098110\,(\text{k}^{-1})$$

$$\Rightarrow \ln\left(\frac{P_1}{P_2}\right) = -3.641; \Rightarrow \ln(P1) - \ln(P2) = -3.641; \Rightarrow \ln(134\text{ mmHg}) - \ln(P2) = -3.641;$$

$\Rightarrow$ 4.897 mmHg – ln(P2) = –3.641; $\Rightarrow$ – ln(P2) = –3.641 – 4.897 mmHg;
$\Rightarrow$ – ln(P2) = – 8.5382; $\Rightarrow$ ln(P2) = 8.5382; $\Rightarrow$ P2 = $e^{8.5382}$ mmHg;
$\Rightarrow$ P2 = 5105.12 mmHg (torr); $\Rightarrow$ P2 = 5105.12/760 = 6.717 atm.

To reach the boiling point 40°C of 2 litres volume DCM (WF **124**), about 4.5 minutes time is needed under adiabatic conditions. That means a pressure of 2.5894 atm., reaches according to the Clausius-Clapeyron equation (Eq. 3). However, during experiments, as the pressure in the bottom chamber of the SLAPE solar panel **100** reached 1 bar, the WF **124** was passed to the RMSE **200** that is connected with electric generator **300** with four magnets and two Cu coils using either a 6 mm outer diameter (OD) and 4 mm inner diameter steel pipe.

4. Concluding remarks and future perspectives

The *Semiconductor and Liquid Assisted Photothermal Effect (SLAPE)*" solar panels were designed and fabricated to generate electricity from sunlight by following a new concept that was not reported so far. In this study, the few numbers of SLAPE solar panels fabricated and investigated to establish the proof of concept of this SLAPE mechanism. In the fabrication of SLAPE solar panels with about a

one square meter area, 21 numbers of multicrystalline silicon photovoltaic cells (SPVCs) together with about 2 litres γ-butyrolactone were employed. This latter SLAPE solar panel exhibited about 17 V electricity when attached with a laboratory model reciprocally moved steam engine (RMSE) and a custom-made electric generator. In commercial SPVC solar panels, the 21 number SPV cells generate a maximum voltage of only about 11 V electricity but in this case, these SLAPE solar panels exhibited about 17 V. There a great amount of scope for the improvement of efficiency of these SLAPE solar panels by employing right kinds of components and systems. Further studies are under progress to improve the electricity generating efficiency of the SLAPE solar panels by utilizing improved components and systems such as, better heat-engines, black silicon wafers, and flat-plate double lined vacuum chambers as top-solar glass components. This latter flat-plate vacuum chambers shall work like a wall in the Dewar (i.e., Thermos) flask in terms of arresting the heat-transfer from the SLAPE solar panel into the atmosphere.

Acknowledgements: Author wishes to thank the Department of Science and Technology (DST), New Delhi, Government of India, for Science and Engineering Research Board (SERB)-Empowerment and Equity Opportunities for Excellence in Science (EMEQ) scheme (#SB/EMEQ-218/2014).

References

1. Ganesh, I. (2023) Practicable Artificial Photosynthesis: The Only Option Available Today for Humankind to Make Energy, Environment, Economy and Life Sustainable on Earth, *Book published by White Falcon Publishers ISBN Number 978-1-63640-828-6*, 1-716.
2. Olah GA, Goeppert A, Prakash GKS. Chemical recycling of carbon dioxide to methanol and dimethyl ether: from greenhouse gas to renewable, environmentally carbon neutral fuels and synthetic hydrocarbons. J Org Chem 2009;74:487-98.
3. Olah GA. Beyond oil and gas: the methanol economy. Angew Chem Int Ed 2005;44:2636-9.
4. Schreier M, Curvat L, Giordano F, Steier L, Abate A, Zakeeruddin SM, Luo J, Mayer MT, Gratzel M. Efficient photosynthesis of carbon monoxide from CO_2 using perovskite photovoltaics. Nat Commun 2015;6.
5. Inoue T, Fujishima A, Konishi S, Honda K. Photoelectrocatalytic reduction of carbon dioxide in aqueous suspensions of semiconductor powders. Nature 1979;277:637-8.
6. Barton EE, Rampulla DM, Bocarsly AB. Selective solar-driven reduction of CO_2 to methanol using a aatalyzed *p*-GaP based photoelectrochemical cell. J Am Chem Soc 2008;130:6342-4.
7. Seshadri G, Lin C, Bocarsly AB. A new homogeneous electrocatalyst for the reduction of carbon dioxide to methanol at low overpotential. J Electroanal Chem 1994;372:145-50.
8. Haas T, Krause R, Weber R, Demler M, Schmid G. Technical photosynthesis involving CO_2 electrolysis and fermentation. Nat Catal 2018;1:32-9.
9. Handoko AD, Wei F, Jenndy YBS, Seh ZW. Understanding heterogeneous electrocatalytic carbon dioxide reduction through operando techniques. Nat Catal 2018;1: 922-34.
10. 10] Centi G, Perathoner S. CO_2-based energy vectors for the storage of solar energy. Greenhouse Gas Sci Technol 2011;1:21.
11. Centi G, Perathoner S. Towards solar fuels from water and CO_2. ChemSusChem 2010;3:195-208.
12. Centi G, Perathoner S. Opportunities and prospects in the chemical recycling of carbon dioxide to fuels. Catal Today 2009;148:191-205.
13. Medina-Ramos J, Pupillo RC, Keane TP, DiMeglio JL, Rosenthal J. Efficient conversion of CO_2 to CO using tin and other inexpensive and easily prepared post-transition metal catalysts. J Am Chem Soc 2015;137:5021-7.
14. Medina-Ramos J, DiMeglio JL, Rosenthal J. Efficient reduction of CO_2 to CO with high current density using in situ or ex situ prepared Bi-based materials. J Am Chem Soc 2014;136:8361-7.
15. Asadi M, Kumar B, Behranginia A, Rosen BA, Baskin A, Repnin N, Pisasale D, Phillips P, Zhu W, Haasch R, Klie RF, Král P, Abiade J, Salehi-Khojin A. Robust carbon dioxide reduction on molybdenum disulphide edges. Nat Commun 2014;5.
16. Rosen BA, Haan JL, Mukherjee P, Braunschweig B, Zhu W, Salehi-Khojin A, Dlott DD, Masel RI. In situ spectroscopic examination of a low overpotential pathway for carbon dioxide conversion to carbon monoxide. J Phys Chem C 2012;116:15307-12.

17. Rosen BA, Salehi-Khojin A, Thorson MR, Zhu W, Whipple DT, Kenis PJA, Masel RI. Ionic liquid–mediated selective conversion of CO_2 to CO at low overpotentials. Sci 2011;334:643-4.
18. Ganesh I. BMIM-BF_4 RTIL: synthesis, characterization and performance evaluation for electrochemical CO_2 reduction to CO over Sn and $MoSi_2$ cathodes. C - J Carbon Res 2020;6:47.
19. Ganesh I. BMIM–BF_4 mediated electrochemical CO_2 reduction to CO is a reverse reaction of CO oxidation in air—experimental evidence. J Phys Chem C 2019;123:30198-212.
20. Ganesh I. Chapter 4 - the electrochemical conversion of carbon dioxide to carbon monoxide over nanomaterial based cathodic systems: measures to take to apply this laboratory process industrially. In Applications of Nanomaterials (Mohan Bhagyaraj, S., Oluwafemi, O. S., Kalarikkal, N., and Thomas, S., Eds.), Woodhead Publishing, 2018;83.
21. Ganesh I. Electrochemical conversion of carbon dioxide into renewable fuel chemicals – The role of nanomaterials and the commercialization. Renew Sustain Energy Rev 2016;59:1269-97.
22. Ganesh I. Solar fuels vis-a´-vis electricity generation from sunlight: the current state-of-the-art (a review). Renew Sustain Energy Rev 2015;44:904-32.
23. Ganesh I, Kumar PP, Annapoorna I, Sumliner JM, Ramakrishna M, Hebalkar NY, Padmanabham G, Sundararajan G. Preparation and characterization of Cu-doped TiO_2 materials for electrochemical, photoelectrochemical, and photocatalytic applications. Appl Surf Sci 2014;293: 229-47.
24. Ganesh I. Conversion of carbon dioxide into methanol – a potential liquid fuel: Fundamental challenges and opportunities (a review). Renew Sustain Energy Rev 2014;31:221-57.
25. Ganesh I. Conversion of carbon dioxide into several potential chemical commodities following different pathways-a review. Mater Sci Forum 2013;764:1-82.
26. Zeng K, Zhang D. Recent progress in alkaline water electrolysis for hydrogen production and applications. Prog Energy Combus Sci 2010;36:307-26.
27. Wikipedia. World energy consumption. 15th September 2017.
28. Wikipedia. Energy policy of India. 15th September 2017.
29. https://www.eia.gov/outlooks/ieo/pdf/0484(2016).pdf (Chapter 1. World energy demand and economic outlook).
30. www.eia.gov/ieo. (International Energy Outlook 2017).
31. Centi G, Perathoner S. Nanocatalysis: a key role for sustainable energy future. In *Nanotechnology in Catalysis*, Wiley-VCH Verlag GmbH & Co. KGaA, 2017:383-400.
32. Zhang S, Sun J, Zhang X, Xin J, Miao Q, Wang J. Ionic liquid-based green processes for energy production. Chem Soc Rev 2014;43:7838-69.
33. Budzianowski WM. Negative carbon intensity of renewable energy technologies involving biomass or carbon dioxide as inputs. Renew Sustain Energy Rev 2012;16:6507-21.
34. Budzianowski WM. Value-added carbon management technologies for low CO_2 intensive carbon-based energy vectors. Energy 2012;41:280-97.
35. Maag G, Steinfeld A. Design of a 10 MW particle-flow reactor for syngas production by steam-gasification of carbonaceous feedstock using concentrated solar energy. Energy Fuels 2010;24:6540-7.
36. Klein A, Koerber C, Wachau A, Saeuberlich F, Gassenbauer Y, Harvey SP, Proffit DE, Mason TO. Transparent conducting oxides for photovoltaics: manipulation of Fermi level, work function and energy band alignment. Mater 2010;3:4892-914.
37. Garcia-Martinez J. Nanotechnology for the Energy Challenge. Wiley-VCH Weinheim, Germany, 2010.
38. Cheng YH, Nguyen VH, Chan HY, Wu JCS, Wang WH. Photo-enhanced hydrogenation of CO_2 to mimic photosynthesis by CO co-feed in a novel twin reactor. Appl Energy 2015;147:318-24.
39. Ganesh I. The latest state-of-the-art on artificial photosynthesis. Chem Express 2014;3:131-48.
40. Smieja JM, Benson EE, Kumar B, Grice KA, Seu CS, Miller AJM, Mayer JM, Kubiak CP. Kinetic and structural studies, origins of selectivity, and interfacial charge transfer in the artificial photosynthesis of CO. Proc Natl Acad Sci USA 2012;109:15646-50.
41. Concepcion JJ, House RL, Papanikolas JM, Meyer TJ. Chemical approaches to artificial photosynthesis. Proc Natl Acad Sci USA 2012;109:15560-4.
42. Nazimek D, Czech B. Artificial photosynthesis - CO_2 towards methanol. IOP Conf Ser: Mater Sci Eng 2011;19.
43. Yang CC, Yu YH, van der Linden B, Wu JC, Mul G. Artificial photosynthesis over crystalline TiO_2-based catalysts: fact or fiction? J Am Chem Soc 2010;132:8398-406.
44. Hammarström L, Hammes-Schiffer S. Guest editorial: artificial photosynthesis and solar fuels. Acc Chem Res 2009;42:1859-60.
45. Gust D, Moore TA, Moore AL. Solar Fuels via Artificial Photosynthesis. Acc Chem Res 2009;42:1890-8.
46. Gratzel M, Kalyanasundaram K. Artificial photosynthesis: efficient dye-sensitized photoelectrochemical cells for direct conversion of visible light to electricity. Curr Sci 1994;66:706-14.
47. Hynninen PH. Functions of chlorophylls in photosynthesis. Kem Kemi 1990;17:241-9.
48. https://www.ndtv.com/chennai-news/2015-chennai-floods-a-man-made-disaster-says-cag-report-1881906.

49. https://en.wikipedia.org/wiki/2018_Kerala_floods.
50. Wamsler C, Schäpke N, Fraude C, Stasiak D, Bruhn T, Lawrence M, Schroeder H, Mundaca L. Enabling new mindsets and transformative skills for negotiating and activating climate action: lessons from UNFCCC conferences of the parties. Environ Sci Policy 2020;112:227-35.
51. Sorkar MNI. Framing shaping outcomes: issues related to mitigation in the UNFCCC negotiations. Fudan J Human Social Sci 2020;13:375-94.
52. Prys-Hansen M. Differentiation as affirmative action: transforming or reinforcing structural inequality at the UNFCCC? Global Soc 2020;34:353-69.
53. Oh C. Discursive contestation on technological innovation and the institutional design of the UNFCCC in the new climate change regime. New Political Economy 2020;25:660-74.
54. Broberg M. Interpreting the UNFCCC's provisions on 'mitigation' and 'adaptation' in light of the Paris Agreement's provision on 'loss and damage'. Climate Policy 2020;20:527-33.
55. Teng Y, Zhang D. Long-term viability of carbon sequestration in deep-sea sediments. Sci Adv 2018;4:eaao6588.
56. Sanna A, Uibu M, Caramanna G, Kuusik R, Maroto-Valer MM. A review of mineral carbonation technologies to sequester CO_2. Chem Soc Rev 2014;43:8049-80.
57. Zhu X, Hatzell MC, Logan BE. Microbial reverse-electrodialysis electrolysis and chemical-production cell for H_2 production and CO_2 sequestration. Environ Sci Tech Lett 2014;1:231-5.
58. Hustad CW. Infrastructure for CO_2 collection, transport and sequestration. Trondheim presented at the 3rd Nordic mini-symposium on carbon dioxide storage 2003.
59. Gale J. Using coal seams for CO_2 sequestration. Geologica Belgica 2004;7.
60. Bachu S, Adams JJ. Sequestration of CO_2 in geological media in response to climate change: capacity of deep saline aquifers to sequester CO_2 in solution. Energy Conver Manage 2003;44:3151.
61. Bachu S. Sequestration of CO_2 in geological media: criteria and approach for site selection in response to climate change. Energy Conver Manage 2000;41:953.
62. MatterJM, Stute M, Snæbjörnsdottir SÓ, Oelkers EH, Gislason SR, Aradottir ES, Sigfusson B, Gunnarsson I, Sigurdardottir H, Gunnlaugsson E, Axelsson G, Alfredsson HA, Wolff-Boenisch D, Mesfin K, Taya DFDLR, Hall J, Dideriksen K, Broecker WS. Rapid carbon mineralization for permanent disposal of anthropogenic carbon dioxide emissions. Sci 2016;352:1312-4.
63. Yi Q, Li W, Feng J, Xie K. Carbon cycle in advanced coal chemical engineering. Chem Soc Rev 2015;44:5409-45.
64. Goeppert A, Czaun M, Jones JP, Surya Prakash GK, Olah GA. Recycling of carbon dioxide to methanol and derived products - closing the loop. Chem Soc Rev 2014;43:7995-8048.
65. Tufa RA, Chanda D, Ma M, Aili D, Demissie TB, Vaes J, Li Q, Liu S, Pant D. Towards highly efficient electrochemical CO_2 reduction: cell designs, membranes and electrocatalysts. Appl Energy 2020;277:115557.
66. https://economictimes.indiatimes.com/wealth/fuel-price.
67. https://en.wikipedia.org/wiki/Solar_energy.
68. He J, Liu Y, Liu W, Li Z, Han A, Zhou Z, Zhang Y, Sun Y. The effects of sodium on the growth of Cu(In,Ga)Se_2 thin films using low-temperature three-stage process on polyimide substrate. J Phys D: Appl Phys 2013;47:045105.
69. Kojima A, Teshima K, Shirai Y, Miyasaka T. Organometal halide perovskites as visible-light sensitizers for photovoltaic cells. J Am Chem Soc 2009;131:6050-1
70. Lee CP, Li CT, Ho KC. Use of organic materials in dye-sensitized solar cells. Mater Today 2017;20:267-83.
71. O'Regan B, Gratzel M. A low-cost, high-efficiency solar cell based on dye-sensitized colloidal TiO_2 films. Nat 1991;353:737-40.
72. DiSalvo FJ. Thermoelectric cooling and power generation. Sci 1999;285:703-6.
73. Canavarro D, Chaves J, Collares-Perreira M. New second-stage concentrators (XX SMS) for parabolic primaries: comparison with conventional parabolic trough concentrators. Solar Energy 2013;92:98-105.
74. https://en.wikipedia.org/wiki/Solar_Energy_Generating_Systems.
75. Blakers A, Zin N, McIntosh KR, Fong K. High efficiency silicon solar cells. Energy Procedia 2013;33:1-10.
76. Lorenzi B, Acciarri M, Narducci D. Experimental determination of power losses and heat generation in solar cells for photovoltaic-thermal applications. J Mater Eng Perfor 2018;27:6291-8.
77. Magalhães PMLP, Martins JFA, Joyce ALM. Comparative analysis of overheating prevention and stagnation handling measures for photovoltaic-thermal (PV-T) systems. Energy Procedia 2016;91:346-55.
78. Kinoshita T, Nonomura K, Joong Jeon N, Giordano F, Abate A, Uchida S, Kubo T, Seok SI, Nazeeruddin MK, Hagfeldt A, Gratzel M, Segawa H. Spectral splitting photovoltaics using perovskite and wideband dye-sensitized solar cells. Nat Commun 2015;6:8834.
79. Hosenuzzaman M, Rahim NA, Selvaraj J, Hasanuzzaman M, Malek ABMA, Nahar A. Global prospects, progress, policies, and environmental impact of solar photovoltaic power generation. Renew Sustain Energy Rev 2015;41:284-97.

80. Parida B, Iniyan S, Goic R. A review of solar photovoltaic technologies. Renew Sustain Energy Rev 2011;15:1625-36.
81. Dupeyrat P, Ménézo C, Rommel M, Henning HM. Efficient single glazed flat plate photovoltaic–thermal hybrid collector for domestic hot water system. Solar Energy 2011;85:1457-68.
82. Blankenship RE, Tiede DM, Barber J, Brudvig GW, Fleming G, Ghirardi M, Gunner MR, Junge W, Kramer DM, Melis A, Moore TA, Moser CC, Nocera DG, Nozik AJ, Ort DR, Parson WW, Prince RC, Sayre RT. Comparing photosynthetic and photovoltaic efficiencies and recognizing the potential for improvement. Sci 2011;332:805-9.
83. Parente V, Goldemberg J, Zilles J. Comments on experience curves for PV modules. Prog Photovolt Res Appl 2002;10:571-4.
84. Keshner MS, Arya R. Study of potential cost reductions resulting from super-large-scale manufacturing of PV modules. NREL report NREL/SR-520-36846, 2004.
85. Chen S, Weng J, Huang Y, Zhang C, Hu L, Kong F, Wang L, Dai S. Numerical model analysis of the shaded dye-sensitized solar cell module. J Phys D: Appl Phys 2010;43:305102.
86. Karg F. High efficiency CIGS solar modules. Energy Procedia 2012;15:275-82.
87. Komaki H, Furue S, Yamada A, Ishizuka S, Shibata H, Matsubara K, Niki S. High-efficiency CIGS submodules. Prog Photovoltaics 2012;20:595-9.
88. https://www.pveducation.org/pvcdrom/modules-and-arrays/heat-generation-in-pv-modules.
89. Ganesh I. Surface, structural, energy band-gap, and photocatalytic features of an emulsion-derived B-doped TiO_2 nano-powder. Mol Catal 2018;451:51-65.
90. https://www.securus.lt/what-are-the-most-efficient-solar-panels-of-2019/.
91. https://assets.publishing.service.gov.uk/government/uploads/system/uploads/attachment_data/file/565248/Heat_Pumps_Combined_Summary_report_-_FINAL.pdf.
92. Khandelwal S, Reddy K, Murthy S. Performance of contact and non-contact type hybrid photovoltaic-thermal (PV-T) collectors. Inter J Low-carbon Tech 2007;2:359-75.
93. Barron-Gafford GA, Minor RL, Allen NA, Cronin AD, Brooks AE, Pavao-Zuckerman MA. The photovoltaic heat island effect: larger solar power plants increase local temperatures. Sci Repor 2016;6:35070.
94. Ali A, Ohrdes T, Wagner H, Altermatt PP. Conceptual comparison between standard Si solar cells and back contacted cells. Energy Procedia 2014;55:11-6.
95. Hussain A, Batra A, Pachauri R. An experimental study on effect of dust on power loss in solar photovoltaic module. Renew: Wind, Water, and Solar 2017;4:9.
96. Hogan NJ, Urban AS, Ayala-Orozco C, Pimpinelli A, Nordlander P, Halas NJ. Nanoparticles heat through light localization. Nano Lett 2014;14:4640-5.
97. https://www.sciencedaily.com/releases/2018/04/180419130051.htm.
98. http://www.solarrooftop.gov.in/goa/faq?q=5.
99. Royne A, Dey CJ, Mills DR. Cooling of photovoltaic cells under concentrated illumination: a critical review. Solar Energy Mater Solar Cells 2005;86:451-83.
100. Neumann O, Urban AS, Day J, Lal S, Nordlander P, Halas NJ. Solar vapor generation enabled by nanoparticles. ACS Nano 2013;7:42-9.
101. Pustovalov VK. Light-to-heat conversion and heating of single nanoparticles, their assemblies, and the surrounding medium under laser pulses. RSC Adv 2016;6:81266-89.
102. Kim J, Kim JT. Comparison of electrical and thermal performances of glazed and unglazed PVT collectors. Inter J Photoenergy 2012.
103. Grubišić-Čabo F, Nizetic S, Tina G. Photovoltaic panels: a review of the cooling techniques. Trans FAMENA 2016;40:63-74.
104. Bahaidarah H, Subhan A, Gandhidasan P, Rehman S. Performance evaluation of a PV (photovoltaic) module by back surface water cooling for hot climatic conditions. Energy 2013;59:445-53.
105. Eicker U, Dalibard A. Photovoltaic–thermal collectors for night radiative cooling of buildings. Solar Energy 2011;85:1322-5.
106. Mellor A, Alonso Alvarez D, Guarracino I, Ramos A, Riverola Lacasta A, Ferre Llin L, Murrell AJ, Paul DJ, Chemisana D, Markides CN, Ekins-Daukes NJ. Roadmap for the next-generation of hybrid photovoltaic-thermal solar energy collectors. Solar Energy 2018;174:386-98.
107. Du D, Darkwa J, Kokogiannakis G. Thermal management systems for Photovoltaics (PV) installations: a critical review. Solar Energy 2013;97:238-54.
108. He W, Chow TT, Ji J, Lu J, Pei G, Chan LS. Hybrid photovoltaic and thermal solar-collector designed for natural circulation of water. Appl Energy 2006;83:199-210.
109. Helden W, Ch R, Zolingen V, Zondag H. PV thermal systems: PV panels supplying renewable electricity and heat. Prog Photovoltaics 2004;12.
110. https://www.youtube.com/watch?v=HurYZkqo54Q.
111. https://hardware.slashdot.org/story/17/07/01/0442203/study-claims-discarded-solar-panels-create-more-toxic-waste-than-nuclear-plants.

112. Hernandez RR, Easter SB, Murphy-Mariscal ML, Maestre FT, Tavassoli M, Allen EB, Barrows CW, Belnap J, Ochoa-Hueso R, Ravi S, Allen MF. Environmental impacts of utility-scale solar energy. Renew Sustain Energy Rev 2014;29:766-79.
113. Dubey S, Jadhav NY, Zakirova B. Socio-economic and environmental impacts of silicon based photovoltaic (PV) technologies. Energy Procedia 2013;33:322-34.
114. https://en.wikipedia.org/wiki/Energiewende.
115. https://www.cleanenergywire.org/easyguide.
116. https://www.therebel.media/energiewende_renewable_energy_lessons_from_germany_s_costly_taxpayer_funded_experiments.
117. Gärtner WW. Photothermal effect in semiconductors. Phys Rev 1961;122:419-24.
118. Liu L, Zhu L, Wang Y, Huang Q, Sun Y, Yin Z. Heat dissipation performance of silicon solar cells by direct dielectric liquid immersion under intensified illuminations. Solar Energy 2011;85:922-30.
119. Zhu L, Wang Y, Fang Z, Sun Y, Huang Q. An effective heat dissipation method for densely packed solar cells under high concentrations. Solar Energy Mater Solar Cells 2010;94:133-40.
120. Jackson WB, Amer NM, Boccara AC, Fournier D. Photothermal deflection spectroscopy and detection. Appl Opt 1981;20:1333-44.
121. https://www.kanthal.com/en/products/furnace-products/electric-heating-elements/.
122. Colli AN, Girault HH, Battistel A. Non-precious electrodes for practical alkaline water electrolysis. Mater (Basel) 2019;12:1336.
123. Chou CH, Chen CD, Wang CRC Highly efficient, wavelength-tunable, gold nanoparticle based optothermal nanoconvertors. J Phys Chem B 2005;109:11135-8.
124. Jiang K, Smith DA, Pinchuk A. Size-dependent photothermal conversion efficiencies of plasmonically heated gold nanoparticles. J Phys Chem C 2013;117:27073-80.
125. John SK, John D, Bijoy N, Chathanathodi R, Anappara AA. Magnesium diboride: an effective light-to-heat conversion material in solid-state. Appl Phys Lett 2017;111:033901/033901-033901/033904.
126. Ganesh I. A device and method for converting sunlight into heat energy using semiconducting materials immersed in a stable organic solvent for electricity generation. Indian Patent Application Number # TEMP/E-1/43582/2020-CHE, 10th Sep 2020.
127. Gong K, Fang Q, Gu S, Li SFY, Yan Y. Nonaqueous redox-flow batteries: organic solvents, supporting electrolytes, and redox pairs. Energy Environ Sci 2015;8:3515-30.
128. Izutsu K. Electrochemistry in Nonaqueous Solutions, 2002.
129. Ue M, Ida K, Mori S. Electrochemical properties of organic liquid electrolytes based on quaternary onium salts for electrical double-Layer capacitors. J Electrochem Soc 1994;141:2989-96.
130. Mieloszyk M, Majewska K, Zywica G, Kaczmarczyk TZ, Jurek M, Ostachowicz W. Fibre Bragg grating sensors as a measurement tool for an organic Rankine cycle micro-turbogenerator. Measurement 2020;157:107666.
131. Mott, K. A., and Peak, D. (2011) Alternative perspective on the control of transpiration by radiation, *Proceedings of the National Academy of Sciences of the United States of America 108*, 19820-19823.